Noise measurement and modeling of advanced SiGe and $A_{III}B_V$ HBTs

P. Sakalas[1,2]

[1] Chair for Electron Devices and Integrated Circuits, University of Technology Dresden, Germany, paulius.sakalas@tu-dresden.de

[2] Fluctuation Phenomena Lab., Semiconductor Physics Institute, 2600 Vilnius, Lithuania

MOS -AK, Shanghai, PR of China, June 26 2016

• Outline

- Introduction.
- Intrinsic noise sources relevant for bipolar technology transistors.
- High frequency noise interpretation and measurement techniques.
- Noise parameter determination methods, uncertainty analysis.
- Noise parameter de-embedding from parasitic network.
- Noise modeling, analytical approach, noise in compact model HiCuM.
- Noise parameters in SiGe HBTs over technology node, noise sources decomposition of NF_{min}.
- Shot noise correlation in SiGe HBTs, compact model solution and verification.
- Avalanche multiplication noise in SiGe HBT: measurement and modeling.
- High frequency noise in advanced InP based HBTs: suitability for LNA?
- GaAs HBT: transit time, f_{T}, NF_{min} dependence on base layer thickness, doping.
- Intervalley noise in GaAs HBTs?

Introduction

- SiGe and InP/InGaAs heterojunction bipolar transistor process technology advancements:
  - BiCMOS technologies offer SiGe HBTs with transit frequency f_{max} > 500/670 GHz.(EU DOT5/ DOT7.
  - InP HBTs features f_T > 760 GHz.[W.Snodgrass, IEDM 2006] and f_{max} > 1.1THz GHz.
- Applications of bipolar transistors: high-frequency/high-speed operation.
  - Bluetooth, 802.11, WLAN (e.g. 60 GHz), UWB (impulse) radio, Free Space Optics, OC 192/768...
- High frequency noise is a bottleneck for front-end circuit modules. Efficient circuit design and optimization require accurate compact models capturing the device characteristics over a wide bias, frequency, temperature and geometry ranges, including the h.f. noise.
  - presently: covered by advanced compact models (CM) such as HICUM, MEXTRAM, VBIC
  - increasing importance of accurate modeling of high frequency noise

This tutorial focuses on h.f. noise measurements and modeling for various technology HBTs

- Tutorial **goals**:
  - introduction to noise measurement peculiarities, calculation techniques and modeling issues
  - identification of physical noise mechanisms and causes for possible model weakness
  - evaluation of CM over technology node on SiGe HBTs $\Rightarrow$ discrepancies, solutions?
  - evaluation of CM over $A_{III}B_V$ DHBTs $\Rightarrow$ new physical effects, device scaling, shot noise correlation.

Wireless application spectrum

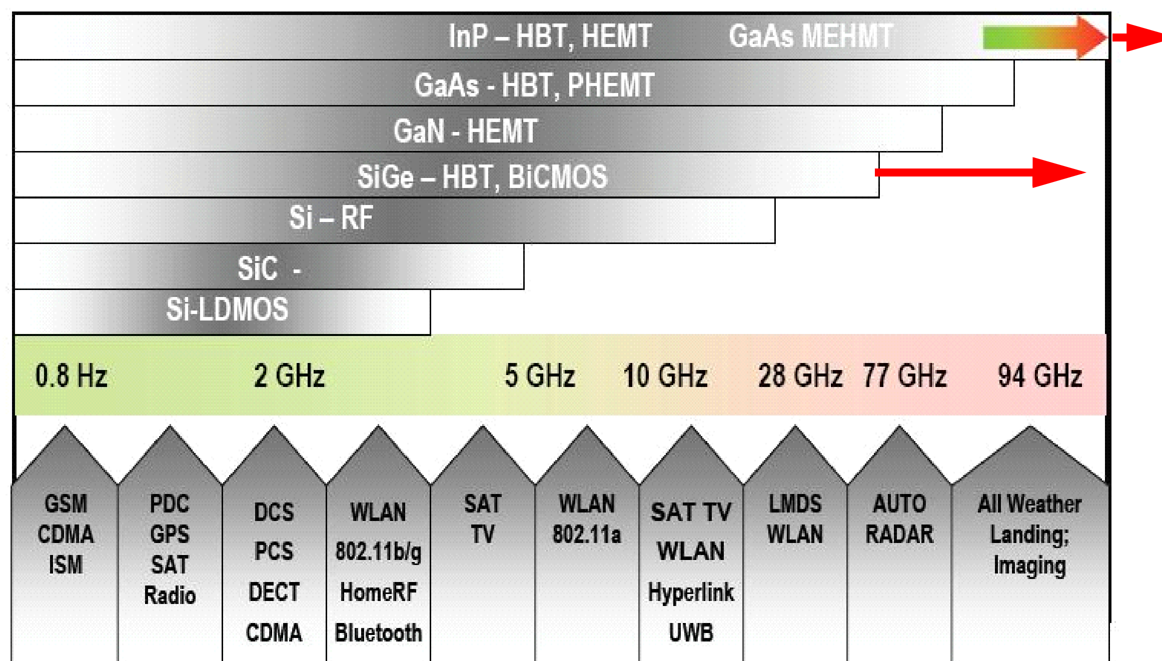

Figure RFAMS1 Wireless Communication Application Spectrum

- Nowadays SiGe technology moved forward yielding f_T = 450 GHz and f_{max} = 670 GHz

•InP DHBTs exhibit f_T = 700 GHz and f_{max} = 1100 GHz

[
0]http://public.itrs.net

ITRS for SiGe and InP HBTs

Table RFAMS7 Millimeter Wave 10 GHz–100 GHz Technology Requirements

Year of Production	*2007*	*2008*	*2009*	*2010*	*2011*	*2012*	*2013*	*2014*	*2015*
InP HBT									
Emitter width (nm)	1	0.5	0.5	0.25			0.13		
Peak F_t (GHz)	150	320		400			560		
Peak F_{max} (GHz)	200	320		560			800		
BV_{ceo}	8	5		4			3		
J_c at Peak F_t (mA/µm^2)	1	5		10			20		
SiGe HBT									
Emitter width (nm)	130	120	100			90			80
Peak F_t (GHz) [V_{bc}=1V]	250	275	300	320	340	360	380	395	415
Peak F_{max} (GHz)	280	305	330	350	370	390	410	425	445
Nfmin (dB) at 60GHz	3.0	2.5	2.2	1.9	1.7	1.5	1.4	1.3	1.2
BV_{ceo}	1.8	1.7	1.65	1.6	1.55	1.5	1.45	1.4	1.35
J_c at Peak F_t (mA/µm^2)	13	15	17	18	19	21	22	23	24

→ 700
1THz

450
670

Manufacturable solutions exist, and are being optimized
Manufacturable solutions are known
Interim solutions are known
Manufacturable solutions are NOT known

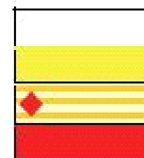

Long term ITRS for SiGe HBTs

Table RFAMS2b RF and Analog Mixed-Signal Bipolar Technology Requirements—Long-term years

Year of Production	*2016*	*2017*	*2018*	*2019*	*2020*	*2021*	*2022*
DRAM ½ Pitch (nm) (contacted)	*22*	*20*	*18*	*16*	*14*	*13*	*11*
General Analog NPN Parameters							
Emitter width (nm) (HS and HV NPN)	80	80	70	70	70	70	70
1/f-noise ($\mu V^2 \cdot \mu m^2/Hz$)	1	1	1	1	1	1	1
σ current matching (%·µm)	2	2	2	2	2	2	2
High Speed (HS) NPN (Common to mmWave Table)							
Peak F_t (GHz) [V_{cb}=1V]	430	445	455	470	480	490	500
Peak F_{max} (GHz)	460	475	485	500	510	520	530
Nfmin (dB) at 60GHz	1.1	1.0	1.0	0.9	0.9	0.9	0.8
BVceo (V)	1.35	1.3	1.3	1.3	1.3	1.25	1.25
J_c at Peak F_t ($mA/\mu m^2$)	25	26	27	28	29	29	30
High Voltage (HV) NPN							
Peak F_t (GHz) [V_{bc}=1V]	130	140	140	150	150	160	160
Peak F_{max} (GHz)	260	270	280	290	300	310	320
BV_{ceo}	2.5	2.4	2.4	2.4	2.4	2.3	2.3
NF_{min} (dB) at 5GHz	<0.2	<0.2	<0.2	<0.2	<0.2	<0.2	<0.2
I_c (µA/µm) at 50GHz F_t	9	8	7	6	5	5	5
Power Amplifier (PA) NPN (Common to PA Table)							
Peak F_t (GHz) [V_{bc}=1V]	40	40	40	40	40	40	40
Peak F_{max} (GHz)	80	80	80	80	80	80	80
Bvceo (V)	7.5	7.5	7.5	7.5	7.5	7.5	7.5
BV_{cbo} (V)	16	16	16	16	16	16	16

Noise maters: limitation of LNA dynamic range

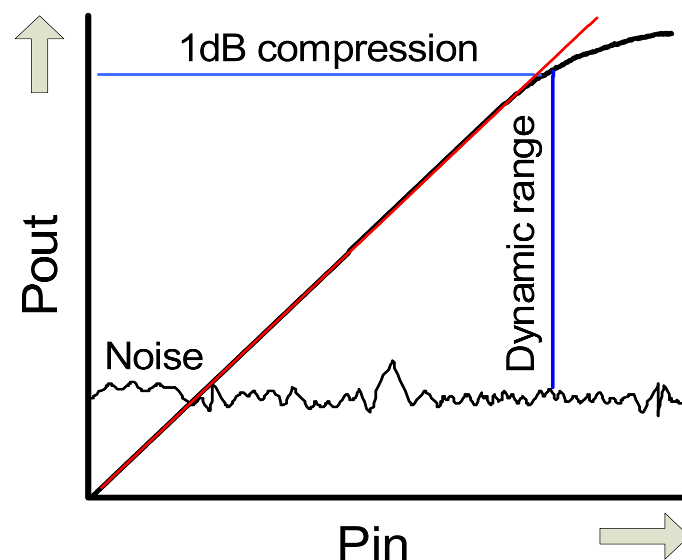

- Important for analog and even digital applications.
- Better dynamic range lower power consumption.
- Benefits for wireless applications: cell phone battery lifetime, distance between base stations.

Intrinsic noise sources

Noise spectra

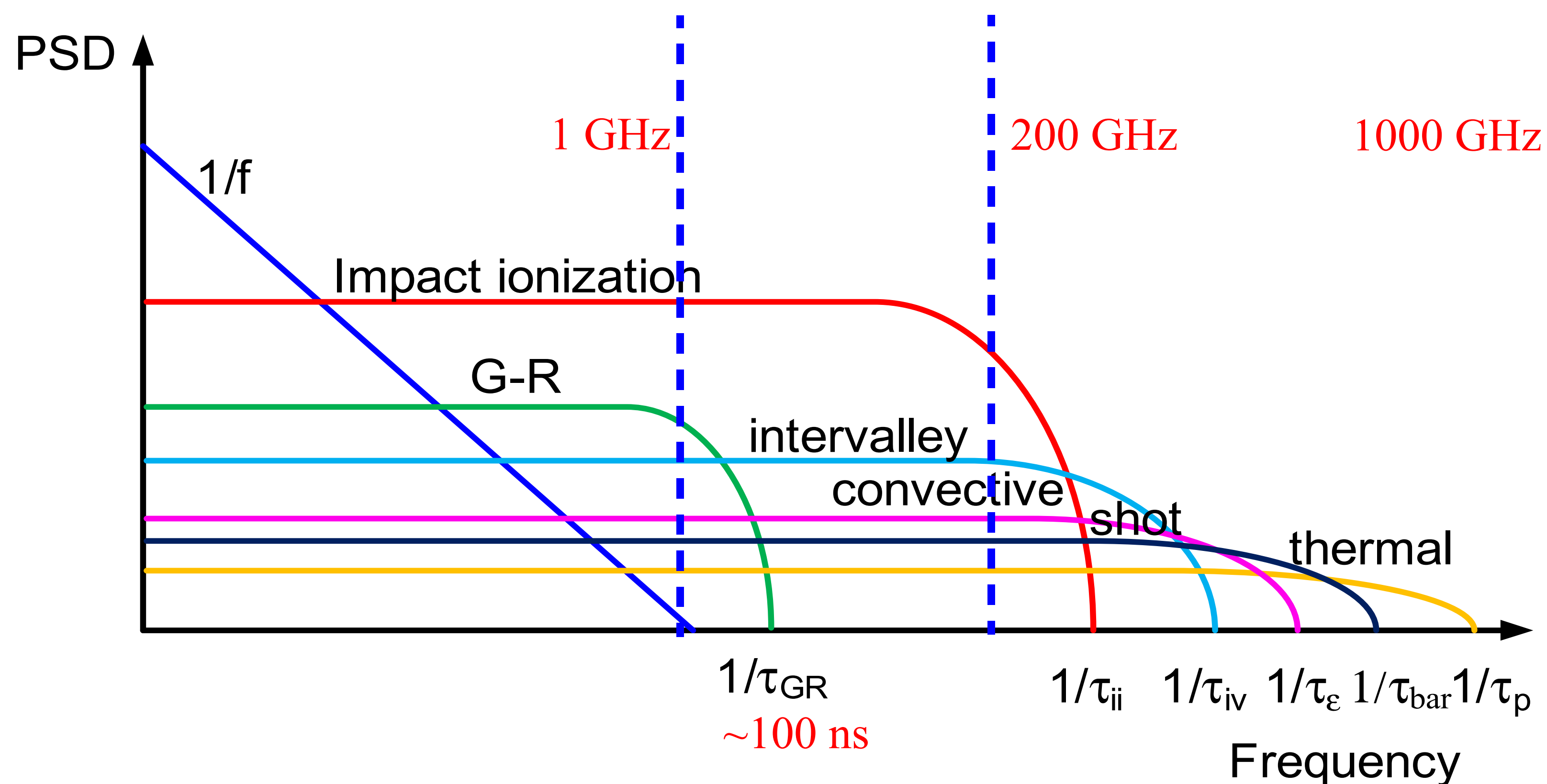

- Depends on lattice temperature and material.
- Practical frequency range high frequency applications lies between blue bars.

Low frequency noise

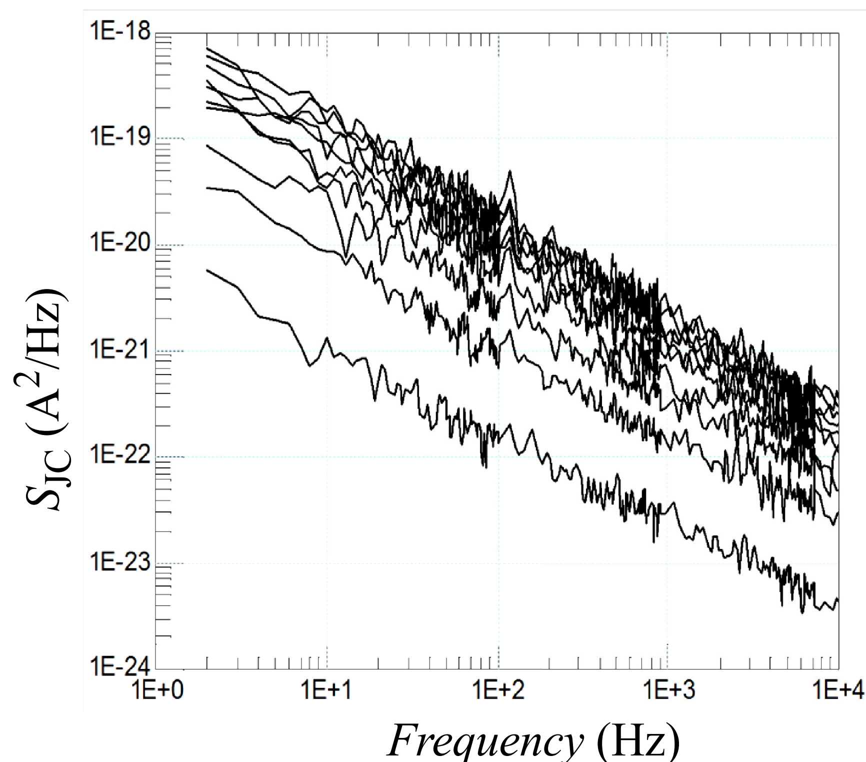

MOSFET

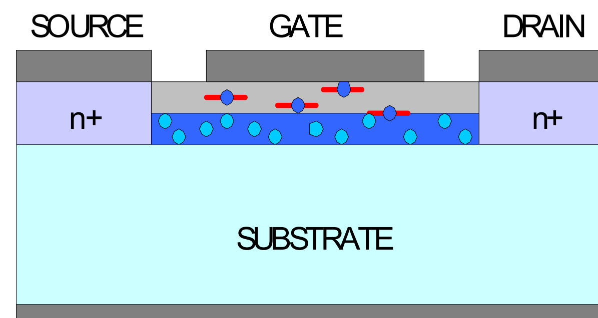

Bipolar

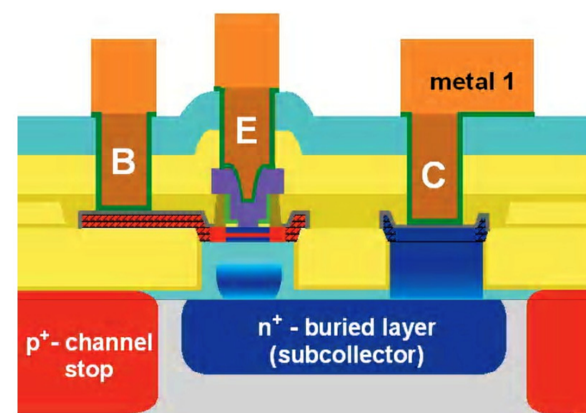

- Collector current flicker noise spectra of SiGe HBT with different bias.
- Typical cut-off frequency lies from 10^{-6} Hz and reaches 100 kHz.
- Two theories behind: 1) Mobility fluctuations, 2) Carrier number fluctuations.

1/f noise: distinguishing between mobility fluctuation and number fluctuation models

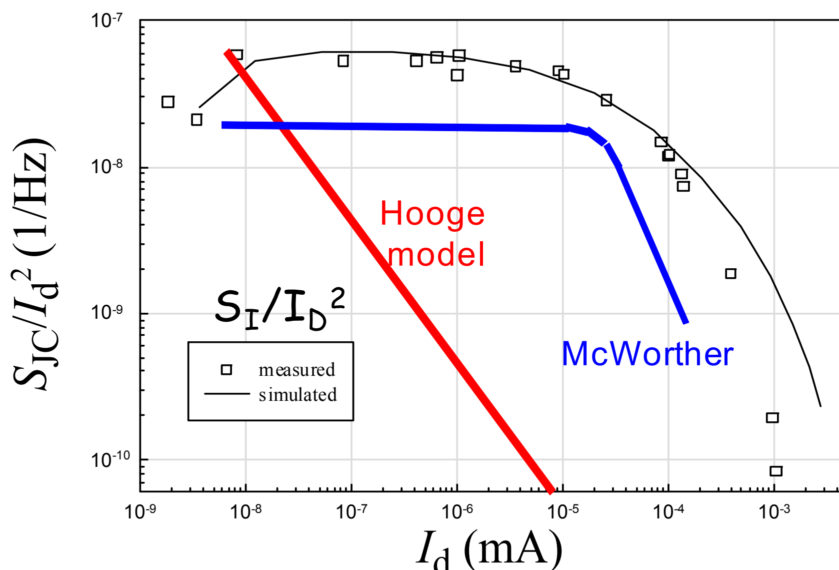

Mobility model $$\frac{S_{I_d}}{I_d^2} \approx \frac{\alpha_H q}{WLQf}$$

Carrier number $$\frac{S_{I_d}}{I_d^2} \approx \frac{g_m^2}{I_d^2} S_{Vfb}$$

$$S_{Vfb} = \frac{q^2 (kT)^2 N_{ST}}{WLC_{OX}^2 f \Delta E_a}$$

- Mobility fluctuation model (Fritz Hooge) implies linear decrease with drain current.
- Carrier number fluctuation model (McWhorter) exhibits square dependent decrease with I_d.
- For planar devices due to numerour defects at the surface McWhorter model is more relevant.
- Bipolar devices are vertical and the Hooge model is dominant in flicker noise.

[2] P.Sakalas, et al, Semiconductor Science and Technology, No.15, pp.799-805, 2000

Generation - Recombination noise

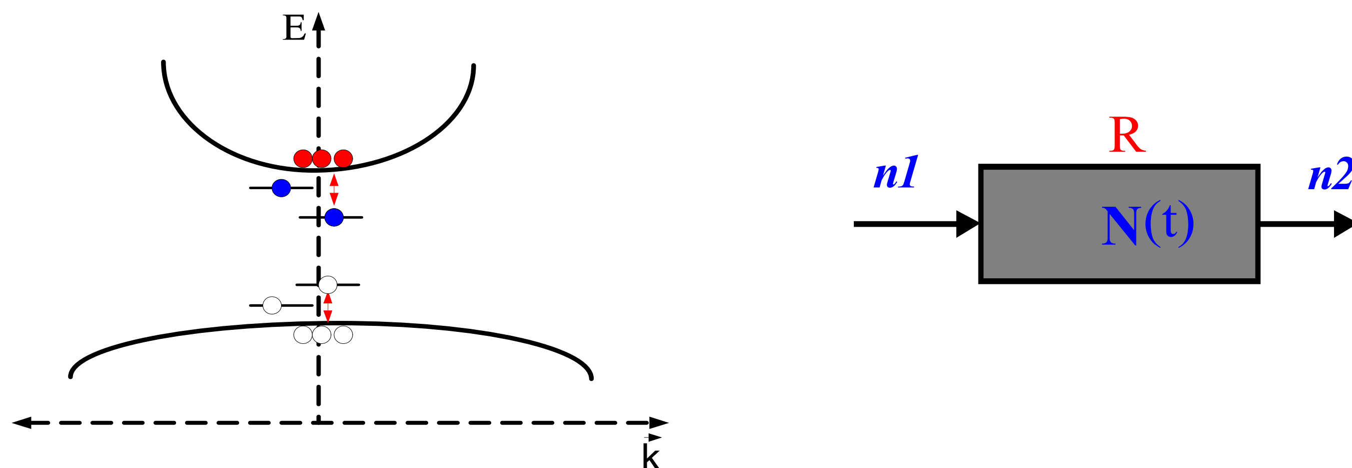

- Ergodic process. Stochastic electron trapping<=> detrapping => to total electron number fluctuations (1951).

- In macroscopic resistor (R) where instanteneous carrier number N(t) fluctuates between 2 levels (conduction band and impurity state) spectral densities are:

$$\frac{S_N(\omega)}{N_0^2} = \frac{S_R(\omega)}{R^2} = \frac{S_G(\omega)}{G^2} = \frac{\overline{\delta N^2}}{N_0^2} \frac{4\tau_N}{(1+\omega^2\tau_N^2)}$$

- Depends on variance of carrier number fluctuations and lifetime of charge carriers. Can be detected when bias is present. Noise spectra is of Lorentzian type.

[3] Noise and Fluctuations Control in Electronic devices, ed. A Balandin, V.Mitin, L. Regiani, L Varani, chapter 2, Generation-Recombination Noise in Semiconductors, 2002

Shot noise

- **Shot noise** is associated with drift of carriers in electric field and is observed in the systems when the particle has to overcome a potential barrier (Schottky, 1918).

=> Present in vaacum tube diodes, p-n junctions, bipolar transistors.

- **Shot noise current spectral density** reads:

$$S_{SH}(\omega) = 4qI\left[\frac{(1-\cos\omega\tau_{bar})}{\omega^2\tau_{bar}^2}\right]$$

- **At lower frequency** $\omega\tau_{bar} << 1$, we have $\cos(\omega\tau_{bar}) = 1+1/2\ \omega^2\tau_{bar}^2 + \ldots$

=> Shot noise becomes white: $S_{SH}(\omega) = 2qI$, where τ_{bar} is barrier crossing time.

=> Shot noise is present if the carrier cross the barrier which energy is $>> kT$.

- **Validity of** $S_{SH}(\omega) = 2qI$: no mutual interaction in between random pulse events.

- **General case:** $S_{SH}(\omega)/\zeta = 2qI$, ζ is a suppresion factor (Fano). Supression appears if:
  - Coulomb short and long range interaction is present
  - Coulomb blocking takes place
  - Correlated currents
  - Related with Pauli principle

[4] M.J.Buckingham, Noise in Electronic Devices and Systems, John Willey & Sons, New York, 1983
[5] A.Reklaitis, L.Regiani, Noise Letters, 1998

Intervalley transfer related noise

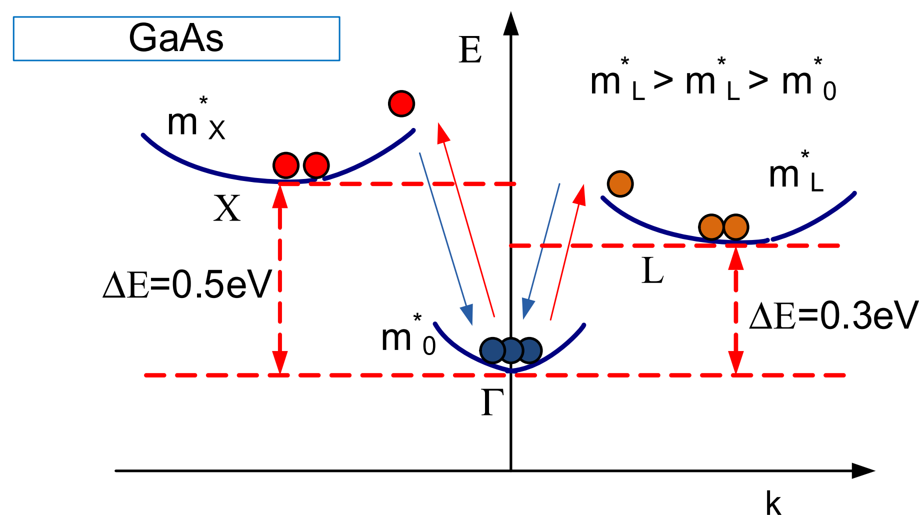

- Random transfer of hot electrons from Γ to L or X valleys featuring different m* and thus drift velocities v_1 and v_2.

$$S_{Iiv}(\omega) \sim \frac{4q^2 n_1 n_2 (v_1 - v_2)^2}{n\tau_{iv}}$$

- For Si intervalley noise (IV) is important only if electric field $E \parallel$ <100> but not for $E \parallel$ <111>.
- For InP and GaAs IV noise is very strong (T_N=3000-5000°K).

[6] P.J. Price "Intervalley Noise", AIP Journal of Applied Physics, vol.31, no.6, pp. 949-953, June 1960.

Thermal noise

For ambient temperature T > 0 K => random motion of electrons with kinetic energy ~ T => voltage fluctuations. Noise voltage => in general case Plank black body radiation law:

$$V_{th}(t) = \sqrt{\frac{4hf_c\Delta fR}{e^{\frac{hfc}{kT}} - 1}}$$

h is Planck's constant, f_c is central frequency of the bandwidth, Δf is bandwidth, R is resistance

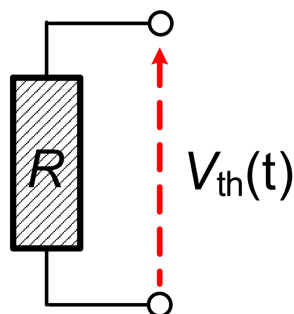

$<V_{th}> = 0$

$\mathrm{rms}(V_{th}) > 0$

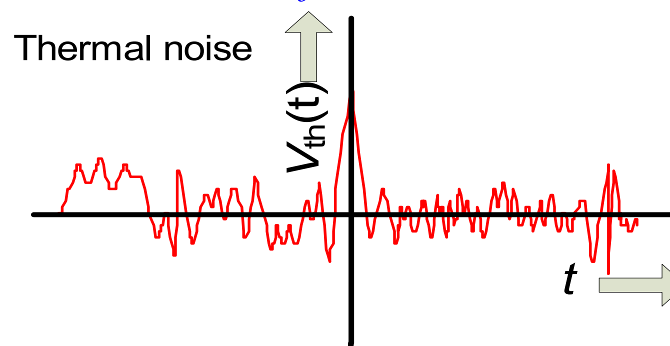

- Worst case: T = 100 K, f_c = 100 GHz: hf = 6.54x10^{-23} << kT = 1.38x10^{-21} then: $e^{\frac{hf_c}{kT}} - 1 \cong \frac{hf_c}{kT}$

and formula simplifies to Rayleigh-Jeans approximation or Johnsons noise: $V_{th}(t) = \sqrt{4TR\Delta f}$

- For microwave frequencies and at practical temperatures a simplified formula can be used.

- At T = 4 K, f_c = 100 GHz, hf_c = 6.5x10^{-23} =~ kT = 5.5x10^{-23} => approximation is not valid.

[7] A.Van der Ziel, Fluctuation Phenomena in Semiconductors, 1959, [
8] D.V.Pozar, Microwave Engineering, John Willey & Sons, New York, 1998

H. F. Noise interpretation and measurement techniques

Thermal noise power in two terminal devices

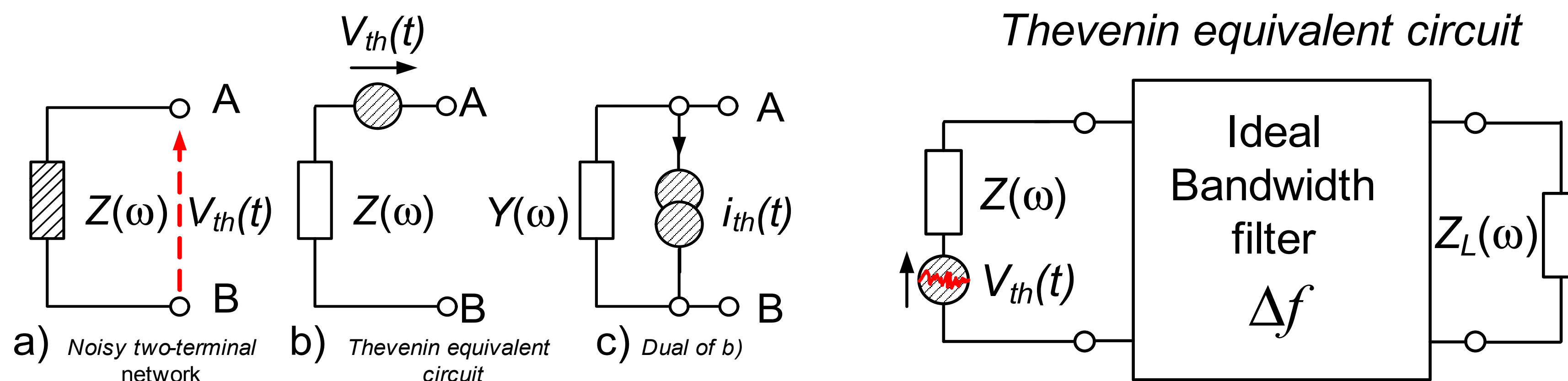

- Three noise in resistor representations. Usefull representation: b) Thevenin.
- Usefull way of stating Nyquist's theorem is noise power in the bandwidth Δf. Then noise power delivered to the load $Z_L(\omega)$ via filter Δf is: $P_n = \left(\frac{V_{th}}{2R}\right)^2 R = kT\Delta f$. Important notes:

a) Δf => 0, P_n => 0, b) T => 0, P_n => 0, c) Δf =>infinity, P_n => infinity (ultraviolet catastrophy)?
=> In case of additional noise sources in $Z(\omega)$ (hot electron, impact ionization or shot noise) Nyquist relation is extended by substituting thermodynamic temperature T with equivalent noise temperature T_n: $P_s = \left(\frac{V_{th}}{2R}\right)^2 R = kT_n\Delta f$. Condition is noise source should be "white".

[7] A.Van der Ziel, Fluctuation Phenomena in Semiconductors, 1959, [8] D.V.Pozar, Microwave Engineering, John Willey & Sons, New York, 1998

Noise in Two Port active network, noise figure

Transistor can be treated as two port network.

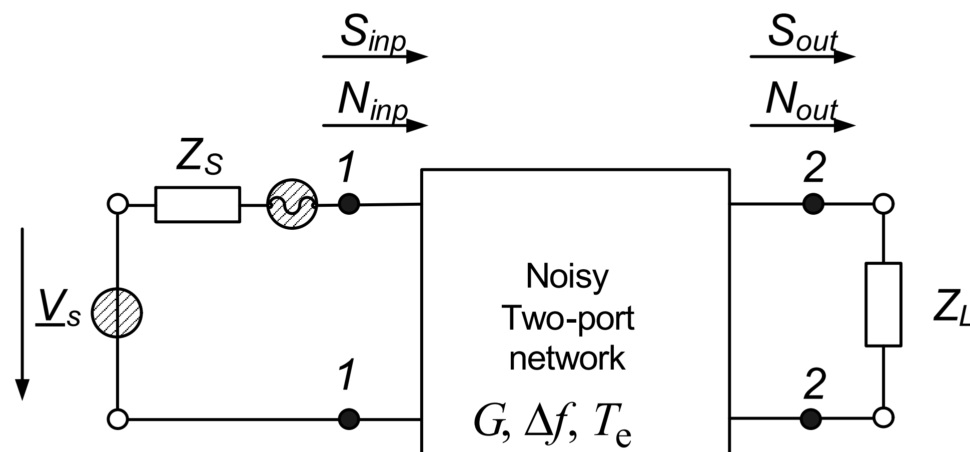

$$F = \frac{S_{inp} / N_{inp}}{S_{outp} / N_{outp}} \geq 1$$

$$F = \frac{S_{inp}}{kT\Delta f} \frac{kG\Delta f (T + T_e)}{GS_{inp}} = \geq 1$$

- Noise Factor was introduced by H. T. Friis for amplifiers. It shows degradation of signal to noise power ratio between the input and output. If two port network is noiseless (T_e=0) then signal and noise will be amplified in a same way without degradation yielding $F = 1$.
- Definition is valid for matched Z_S at $T_0 = 290$ K!
- Noise figure is: $NF = 10 \log F \geq 0$. For passive two port $F = 1 + 1\left((L-1) \cdot \frac{T}{T_0}\right) \geq 0$, where L is loss factor ~1/G. If $T = T_0$ then for 10 dB attenuator F = 10 dB.

[9] H.T.Friis, Proc.IRE v32, pp. 419-422. 1944

Noise parameters, minimum noise figure

Noise figure is affected by the source impedance.

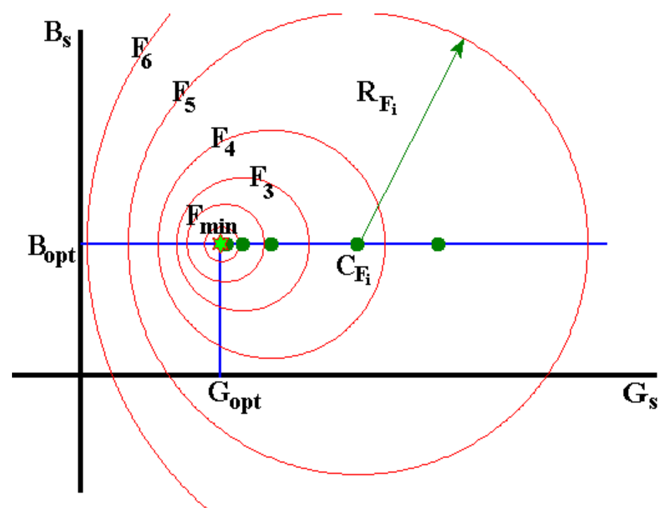

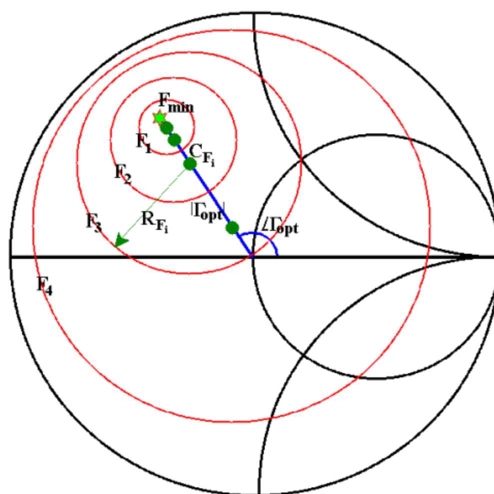

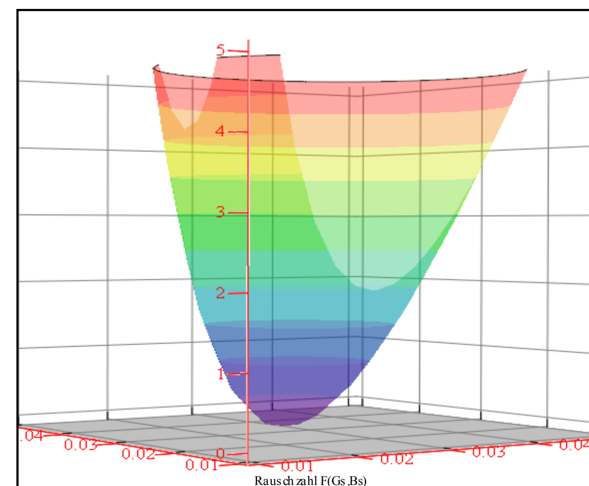

$$NF = NF_{\min} + \frac{R_n}{G_S}\left[(G_S - G_{opt})^2 + (B_S - B_{opt})^2\right]$$

$$NF = NF_{\min} + \frac{4R_n}{Z_0}\frac{\left|\Gamma_S - \Gamma_{opt}\right|^2}{\left|1+\Gamma_{opt}\right|^2\left(1-\left|\Gamma_S\right|^2\right)} \quad \Gamma_S = \frac{(R_S + jX_S) - Z_0}{(R_S + jX_S) + Z_0}$$

Noise parameter scaling

$$R_n^{(m)} = \frac{R_n}{m};$$

$$Y_{Sopt}^{(m)} = mY_{Sopt};$$

$$F_{\min}^{(m)} = F_{\min};$$

$$G_{S\min R}^{(m)} = mG_{S\min R};$$

$$F_{\min R}^{(m)} = F_{\min R}$$

[8] D.V.Pozar, Microwave Engineering, John Willey & Sons, New York, 1998

Noise figure measurement: *Y-Factor* method

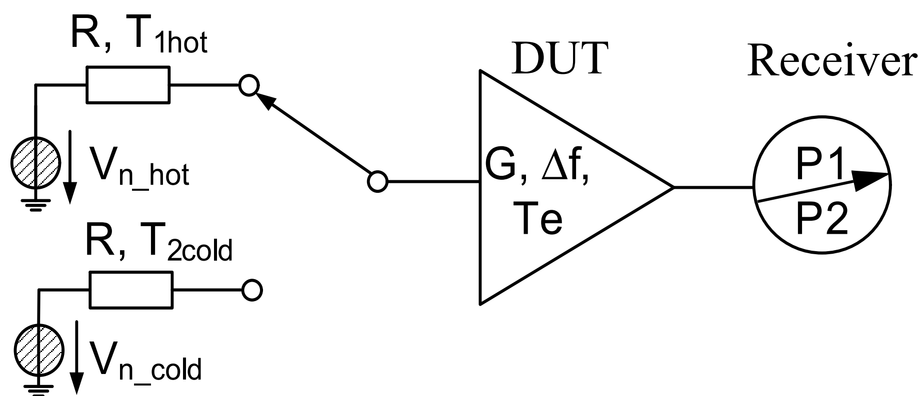

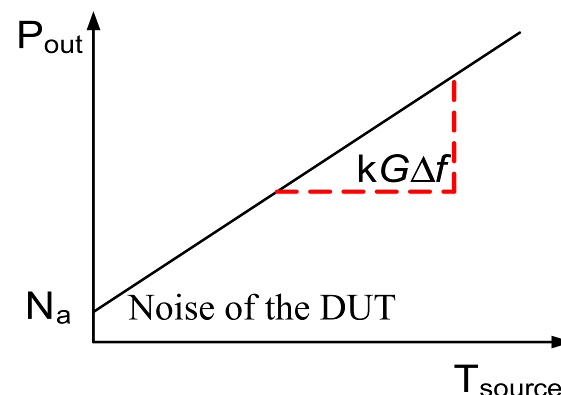

Output power $P1$ and $P2$ consists of:

$P1 = GkT_{1hot}\Delta f + GkTe\Delta f$

$P2 = GkT_{2cold}\Delta f + GkTe\Delta f$ => two unknowns: G x Δf product and Te. Defining $Y = \frac{P1}{P2} = \frac{T_{1hot} + Te}{T_{2cold} + Te}$ and resolving for Te: $T_e = \frac{T_{1hot} - YT_{2cold}}{Y - 1}$

- T_{1hot} and T_{2cold} should not be close and R should be well matched. Usually a noise source is used in *hot* and *cold* states with an excess noise ration (ENR): $ENR_{dB} = 10\log\left(\frac{T_{1hot} - T_{2cold}}{T_0}\right)$

=> **General assumption is**: bandwidth Δf of the DUT should exceed receivers bandwith. P_{out} of the DUT should be linear in reference of source noise power.

Drawback: reflections of the receiver are not accounted.

[8] D.V.Pozar, Microwave Engineering, John Willey & Sons, New York, 1998, [10]Agilent Application note 57-1, Fundamentals of Microwave Noise Measurements, [11]J. P .Dunsmore, Handbook of Microwave Component Measurements with advanced VNA techniques, Willey 2012.

Noise receiver calibration

System noise can be obtained from ENR at ***hot*** and ***cold*** measurements:

$$NF_{Sys} = \frac{ENR - Y}{Y - 1} \text{, where } Y = \frac{P1}{P2} = \frac{P_{hot}}{P_{cold}}$$

ENR is normally defined for ambient temperature T_0 = 290 K. If $T_{2cold} > T_0$ the corrections are required in order to calculate the system noise.

$$NF_{Sys} = \frac{ENR - Y \cdot \left(\frac{T_{2cold}}{T_0} - 1\right)}{Y - 1}$$

Noise system calibration includes the knowledge of receiver noise contribution to all measured noise. If noise of the system and ENR are known then gain and bandwidth of the noise system can be expressed:

$$G\Delta f_{Rec} = \frac{T_{hotRec}}{ENR \cdot T_0 + T_C + T_{Sys}}$$

The corrected actual noise temperature T_A after receiver noise correction with T_{Sys} is:

$$T_A = \frac{T_{MRec}}{G\Delta f_{Rec}} - T_{Sys} \quad ,$$

where T_{MRec} is a raw measured data on the receiver. This correction removes second stage noise contribution.

[11]J. P .Dunsmore, Handbook of Microwave Component Measurements with advanced VNA techniques, Willey 2012.

Noise figure calculation of DUT from *Y-Factor* method

For the connected DUT to the system the Noise figure of the DUT and the system can be expressed:

$$NF^{DUT}{}_{Sys} = \frac{ENR - Y_{DUT} \cdot \left(\frac{T_{2cold}}{T_0} - 1\right)}{Y_{DUT} - 1}, \quad Y_{DUT} = \frac{P_{hotDUT}}{P_{coldDUT}}$$

Applying Friis formulation the system noise can be removed:

$$NF^{DUT} = NF^{DUT}{}_{Sys} - \frac{(NF_{Sys} - 1)}{G_{DUT}}$$

The gain G_{DUT} of can be found from two sets of noise power measurements, *hot* and *cold*:

$$G_{DUT} = \frac{P_{hotDUT} - P_{coldDUT}}{P_{hotRec} - P_{coldRec}}$$

- *Y-Factor* method measures noise figure of the DUT in the impedance of noise source, which is not always 50 Ω. => therefoe G_A diff ers from *S*.21 since it is insertion gain of DUT.
- Preference is ENR use for *Y-Factor* method with not high values to maintain linearity of the receiver (error source).
- *NF* of DUT should not be significant larger that ENR=> too see *hot* and *cold* noise powers.
- Drawback: source reflection coefficient Γ_s from *hot* and *cold* states remains the same.

[11]J. P .Dunsmore, Handbook of Microwave Component Measurements with advanced VNA techniques, Willey 2012

Noise figure measurement: *Cold-Source* method

Differnet form *Y-Factor* method available gain G_A in *Cold-Source* method is calculated from *S*-parameters and knowledge of source impedance. Receiver is calibrated by measuring available noise power $kT_{AOut}\Delta f$ relative to $kT_0\Delta f$. Noise figure can be expressed as:

$NF = 10\log\left(\frac{S_{Inp}/N_{Inp}}{S_{Out}/N_{Out}}\right) = 10\log\left(\frac{T_{AOut}}{T_0 G_A}\right)$, where T_{Aout} is available noise and G_A is available gain.

Gain bandwidth product of the receiver should be pre-characterized. This is done by using noise source measurement in *hot* and *cold* states. Then *NF* is computed: $NF = \frac{T_{Aout}}{G_A \cdot T_0}$, this can be converted to *S*-parameters and incident noise power T_{inc}:

$NF = \frac{T_{Aout}}{G_A \cdot T_0} = \frac{T_{inc}}{T_0} \cdot \frac{|1-\Gamma_S S_{11}|^2}{(1-|\Gamma_S|^2)\cdot|S_{21}|^2}$, where $\frac{T_{inc}}{T_0}$ is DUT related incident power => $\frac{T_{inc}}{T_0} = \frac{T_{Aout}}{T_0} \cdot |1-\Gamma_2|^2$

, where Γ_2 is output match of the device, connected to noise receiver. For matched VNA source impedance to 50 Ω, Noise Figure is:

$NF = \frac{T_{Aout}}{T_0} \cdot \frac{1}{|S_{21}|^2}$ and noise figure in dB: $NF_{dB} = DUTRNP - S_{21dB}$, where *DUTRNP* is relative noise power of the DUT.

[11]J. P .Dunsmore, Handbook of Microwave Component Measurements with advanced VNA techniques, Willey 2012

Noise figure measurement: *Twice Power* method

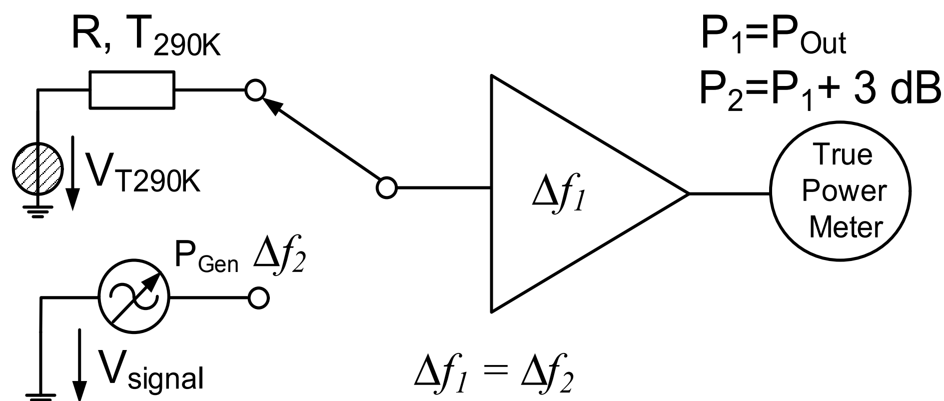

Suitable for high noise DUTs.

- Output power or noise power are measured with load at 290 K at the device input.
- Output power of signal generator (P_{Gen}) at same Δf is measured with adjusted power to 3 dB increase in the output power.
- Generator power level P_{Gen} and Δf should be known then: $F = \frac{P_{Gen}}{kT_0 \Delta f}$

Drawback:

Noise bandwidth of the power measurement device should be known (requires VNA).
True power measurement device needed due to mixed noise and CW power signal.
Power meter (low sensitivity at low noise levels), Spectrum analyzer has good sensitivity and frequency resolution but needs special detector for CW and noise power to be combined.

[10]Agilent Application note 57-1, Fundamentals of Microwave Noise Measurements

Noise figure measurement: *Direct Noise* method

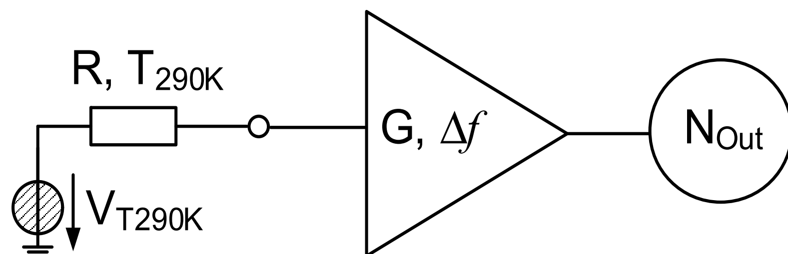

Suitable for high noise DUTs.

- Output noise power of the DUT with input termination at T_0 = 290 K is measured.
- DUT gain G and bandwidth Δf should be known.

$$F = \frac{N_{Out}}{kT_0 G \Delta f}$$

Drawback:

Very accurate terminal noise power measurement device with absolute accuracy is required. Bandwidth and DUT gain must be known.

Notes:

Measures the total noise including system noise => if DUT G is large the system noise has a little impact on noise factor: $F_1 = F - \frac{F_{Sys} - 1}{G}$. Two unkowns G and F_{Sys} can be found from the additional noise source measurement. This is called noise system calibration.

[10]Agilent Application note 57-1, Fundamentals of Microwave Noise Measurements

Noise parameter determination methods

Orthodox method

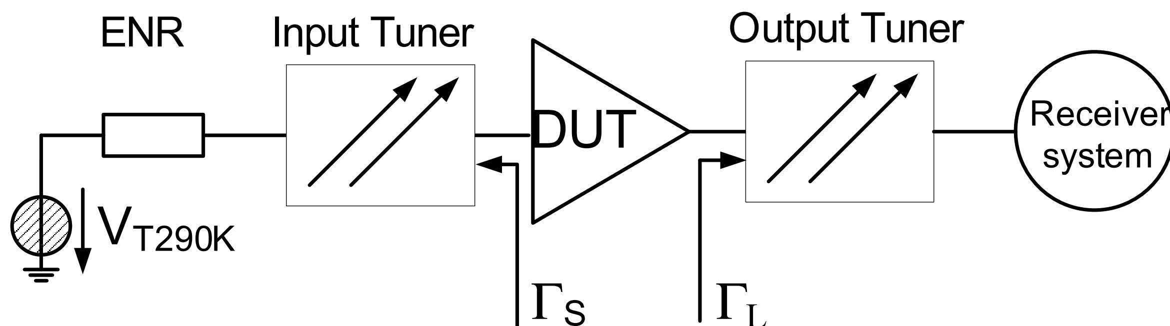

1. Adjust inp. tuner for min F.
2. Adjust out. tuner for max G.
3. Measure F_{min} and Γ_{opt}.
4. Measure another F at another Γ_S.
5. Calculate R_n.

- One of the first measurement methods. Two tuners are required.
- NF_{min} and Γ_{opt} are found by direct search, R_n is found from measurement at different Γ_S:

$$R_n = \frac{F(\Gamma_S) - F_{min}(1 - |\Gamma_S|^2)}{4} \cdot \frac{|1 - \Gamma_{opt}|^2}{|\Gamma_{opt} - \Gamma_S|^2}$$

- Output tuner adjustment makes insertion gain that the noise figure meter allways measures equal to available gain. Then removal of the 2nd stage noise is correct.

Drawback:

Γ_S variation results in gain variations, tuner losses not accounted, input tuner reduces ENR, out. tuner losses adds to F, Available gain depends on Γ_L and DUT and on Γ_S. Maximum gain and minimum noise figure are not independent (isolator between DUT and receiver is an option for improvement).

[12] R. Tuitelaars, "Device noise parameter measurement basics",BSW Test Systems and Consulting Notes.

Noise parameter determination: "*Computational* method"

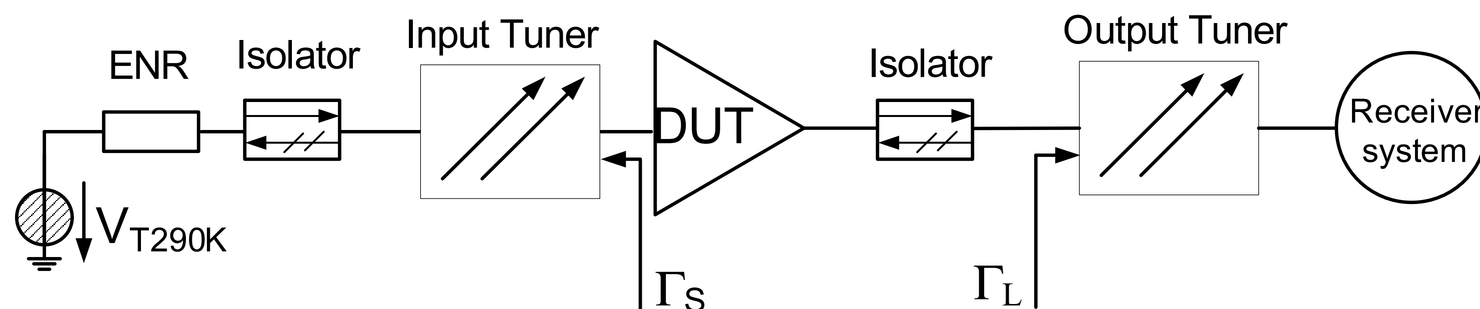

- Similar setup but with isolators at input and output to reduce uncertainties.

Procedure:

- Measure F_i at few (> 4) different $\Gamma_{S,i}$.
- Calculate noise parameters in a least-squares sense from set of F_i and $\Gamma_{S,i}$.
- Calculate output tuning Γ_L and available gain $G_{A,i}$ from measured S-parameters.

Advantages: Accuracy enhancement compared to Orthodox method.

Drawback:

- Requires automation (automated tuner control) and high CPU time (numerical instability).
- Impedance tuners have to be pre-characterized.
- Influence of source reflection change due to diode switching $\Delta\Gamma_S$ is not removed.

[12] R. Tuitelaars, "Device noise parameter measurement basics",BSW Test Systems and Consulting Notes.

Noise parameter determination: "*Linearization* method"

Equation $F(\Gamma_S) = F_{min} + \frac{4R|\Gamma_{opt} - \Gamma_S|^2}{(1 - |\Gamma_S|^2) \cdot (1 - |\Gamma_{opt}|^2)}$ can be linearized and solved by least-square solver.

$$=> \quad F(\Gamma_S) = a + b \cdot \frac{1}{1 - \rho_s^2} + c \cdot \frac{\rho_s \cdot \cos\theta_S}{1 - \rho_s^2} + d \cdot \frac{\rho_s \cdot \sin\theta_S}{1 - \rho_s^2} \quad ,$$

Reflection coefficients are written as: $\Gamma_X = \rho_X \cdot \cos\theta_X + j \cdot \rho_X \cdot \cos\theta_X$.

Parameters a, b, c, d are: $a = F_{min} - \frac{4R}{1 - \rho_{opt}}$, $b = \frac{1 + \rho_{opt}^2}{1 - \rho_{opt}^2}$, $c = \frac{-8R\rho_{opt}\cos\theta_{opt}}{1 - \rho_{opt}^2}$, $d = \frac{-8R\rho_{opt}\sin\theta_{opt}}{1 - \rho_{opt}^2}$

Linear equation can be solved by least square solver sense by solving for a, b, c and d.

Least-squares sense is minimization of error-functions: $\varepsilon = \frac{1}{2}\sum_{i=1}^{n}(F_{Calc} - F_{Meas})^2$

Drawback:

- Under $Z = 0$ for all $\Gamma_{s,i}$ solution fails.
- Must be enough variation in all F_i.
- F_i and G_A tend to +infinity and -infinity respectively for $|\Gamma_s|$ => 1.
- Still lots of research for improvements.

[12] R. Tuitelaars, "Device noise parameter measurement basics",BSW Test Systems and Consulting Notes.

Noise parameter determination: *Adamian-Uhlir* method

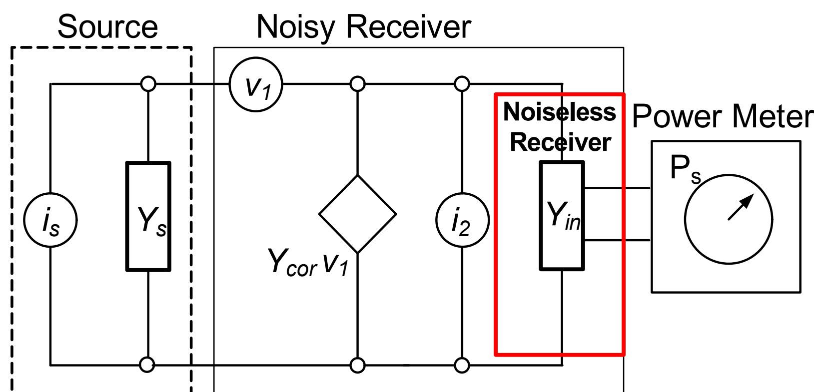

- Representation of noisy receiver follows from Rothe and Dalke: $i_1 = Y_{cor} \cdot v_1 = (G_{cor} + j \cdot B_{cor}) \cdot v_1$, where Y_{cor} is a complex number representing correlation.

Measured noise power absorbed by admittance Y_{in}:

$$P_S = \frac{4kT_0 \Delta f K G_{in}}{|Y_s + Y_{in}|^2} \cdot \left(|Y_s + Y_{in}|^2 \cdot R_n + G_n + G_s \frac{T_s}{T_0} \right)$$

- 5 Unknowns: R_n, G_n, G_{in}, B_{in} and ΔfK (K is newly introduce proportionality coefficeint for gain).
- Requires measurement of input admittance Y_{in} and change of source temperature => measure P_{Shot} and P_{Scold} at first $Y_{s,1}$ with $T_S = T_{hot}$ and $T_S = T_{cold}$ and from $P_{Shot} - P_{Scold} = \frac{4kT_0 \Delta f K G_{in} G_1 (T_{hot} - T_{cold})}{|Y_{s1} + Y_{in}|^2}$ calculate ΔfK.

[13] V. Adamian, A. Uhlir jr, AA Novel Procedure for Receiver Noise Characterization", IEEE Transaction on Instrumentation and Measurement, Vol. IM-22.No.2, pp. 181-182, 1973, [14] H. Rothe, W. Dahlke, “Theory of Noisy Fourpoles,” Proc. *IRE*, 44, pp.811-818, 1956.

Adamian-Uhlir **method** continued

- Measure $P_{S,i}$ at $Y_{s,i}$, i = 1, 2, 3,... at T_S=T_{cold}
- Solve a set of linear equations for A, B, C, D: $A+|Y_{si}|^2 B+2G_{si}C+2B_{si}D=\frac{|Y_{si}+Y_{in}|^2}{(4k\Delta f K G_{in})}\cdot P_{si}-\frac{T_{cold}}{T_0}G_{si}$, where $A=G_n+|Y_{in}|\cdot R_n$, $B=R_n$, $C=G_{in}R_n$, $D=B_{in}R_n$
- The data are collected and solved by least square sense method resulting to noise parameters of the receiver. For data collection for receiver calibration a "thru" is used as DUT.
- The last step is to remove receiver noise parameters as 2nd stage correction from DUT.

Advantages:

- Influence of source reflection change due to diode switching $\Delta\Gamma_S$ is corrected.
- Only 1 tuner at port 2 is needed => reduces system noise.
- Solved problem with insertion and available gain.
- Mathematically stable solution.

Drawback:

- Required measurement of Y_{in}.
- Complex 2nd stage noise removal algorythm.

[12] R. Tuitelaars, "Device noise parameter measurement basics",BSW Test Systems and Consulting Notes.

Noise parameter measurement uncertainty

Device noise parameters are easy to use but very difficult to measure!

Accuracy of *F* is least understood in RF and microwave measurements [11].

Noise parameter measurement and determination accuracy factors:

- Noise figure measurement accuracy: good if *ΔF* [+- 0.17 ... 0.5] dB.
- ENR table accuracy, directly translates to noise figure error (not all noise sources are calibrated => sold off-the-shelf with a standard cal table).
- Tuner accuracy and repeatability: good if for $|\Gamma_s|$ < 0.7...0.8 => 60 dB repeatability.
- Noise parameter determination method used (one of the main errors)=> still many research acivity.

- Instrumentation errors usually are small enough compared to ENR related and *noise parameter* determination errors.
- Mismatch between DUT and Receiver error affects *G* but not *F* since it applies for both in a similar way and thus is cancelled.
- The largest error is related to DUT and source mismatch.

[11]J. P .Dunsmore, Handbook of Microwave Component Measurements with advanced VNA techniques, Willey 2012,
[12] R. Tuitelaars, "Device noise parameter measurement basics",BSW Test Systems and Consulting Notes.

Noise parameter measurement uncertainty *continued*

NF_{min} of GaAs based MESFET.

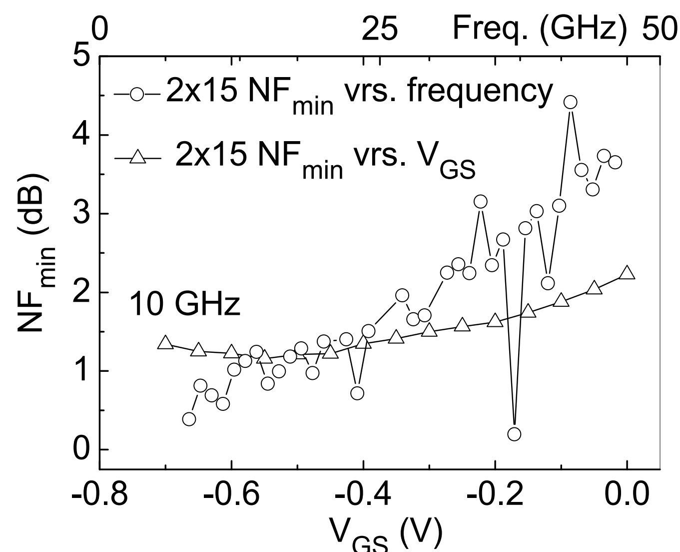

=> Very good repeatability of NF_{min} over V_{GS}

=> Scattered and **very repeatable** data over frequency.

Uncertainties from the equipment are negligible.

Main errors are related to ENR values and source mismatch.

Gate area device A_{L0} = 0.15um x 2um x 15.

- For any measurement method including *Y-Factor* ENR errors translates direct to noise figure:

$$N_{Fsys} = \frac{ENR - \left(\frac{T_C}{T_0} - 1\right)}{Y - 1}$$

- Extremely accurate *ENR:* Agilent developed SNS series noise sources with a built in attenuator to establish lower mismatch to 50 Ω. [10].

[14] P. Sakalas, M. Schroter, "High frequency noise in MESFETs", Internal RML XMOD report, 2016.
[10]Agilent Application note 57-1, Fundamentals RF and Microwave Noise Measurements

Noise parameter de-embedding

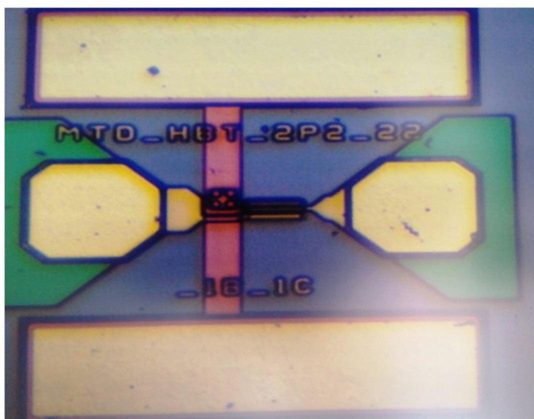

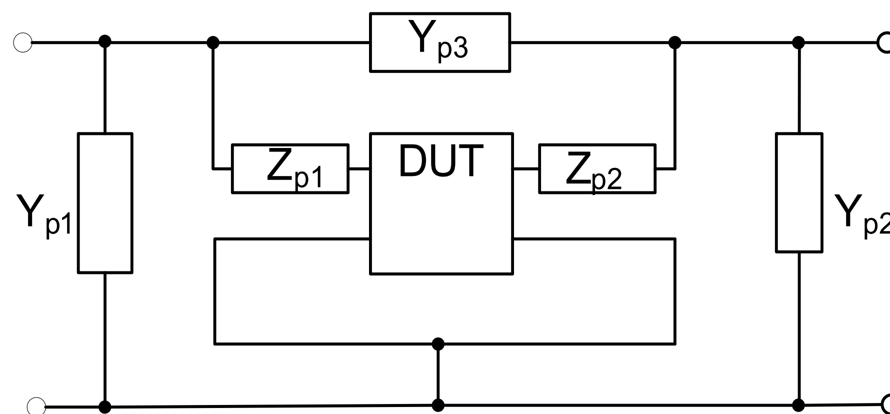

There are few noise de-embedding from the pad parasitic network or fixture techniques:

- Engberg method

- Based on interconnected networks:
  - adjoint networks(for every set of 2-ports all noise contributors are brought to the front of equivalent linear noiseless circuit)
  - Albinson (similar way)
  - correlation matrices (most general method involves lengthy matrix computing) [15].

[12] R. Tuitelaars, "Device noise parameter measurement basics", BSW Test Systems and Consulting Notes.
[15] R. A. Pucel, "A General Noise De-embedding Procedure for Packaged Two-Port Linear Active Devices, IEEE Trans. on MTT, Vol.40, No.11, 1992"

Correlation matrix based noise de-embedding procedure

- Measure the scattering parameters $[S^{DUT}]$ of DUT and "open" structure $[S^{open}]$ => $[Y^{DUT}]$, $[Y^{open}]$.
- Measure noise parameters, NF_{min}^{DUT}, Y_{opt}^{DUT}, R_n^{DUT} => Calculate correlation matrix $[C_A^{DUT}]$:

$$[C_A^{DUT}] = \begin{bmatrix} R_n^{DUT} & \frac{NF_{min}^{DUT}-1}{2} - R_n^{DUT}\cdot(Y_{opt})^* \\ \frac{NF_{min}^{DUT}-1}{2} - R_n^{DUT}\cdot(Y_{opt}) & R_n^{DUT}\cdot(Y_{opt}) \end{bmatrix}$$

- Convert matrix $[C_A^{DUT}]$ to it's correlation matrix $[C_Y^{DUT}]$:

$$[C_Y^{DUT}] = [T^{DUT}][C_A^{DUT}][T^{DUT}]^\dagger, \qquad [T^{DUT}] = \begin{bmatrix} -Y_{11}^{DUT} & 1 \\ -Y_{21}^{DUT} & 0 \end{bmatrix}$$

- Calculate correlation matrix $[C_Y^{open}]$ of the open test structure: $[C_Y^{open}] = 2kTReal([Y^{open}])$.
- Substract paralell parasitics from $[Y^{DUT}]$: $[Y_1^{DUT}] = [Y^{DUT}] - [Y^{open}]$ => $[A] = \begin{bmatrix} Y_{22} & 1 \\ (Y_{11}Y_{22} - Y_{12}Y_{21}) & Y_{11} \end{bmatrix}$
- De-embed $[C_Y^{DUT}]$ from the parallel parasitics: $[C_{Y1}^{DUT}] = [C_Y^{DUT}] - [C_Y^{open}]$ => $[C_A] = [T_A][C_{Y1}^{DUT}][T_A]^\dagger$
- where $[T_A] = \begin{bmatrix} 0 & A_{12} \\ 1 & A_{22} \end{bmatrix}$ => de-embedded noise parameters:

$$F_{minde} = 1 + \frac{1}{kT}Real(C_{12A}) + \sqrt{C_{11A}C_{22A} - (Imag(C_{12A}))^2}, \quad R_{nde} = \frac{C_{11A}}{2kT}$$

$$Y_{optde} = \frac{\sqrt{C_{11A}C_{22A} - (Imag(C_{12A}))^2} + i\cdot Imag(C_{12A})}{C_{11A}}$$

[15] R. A. Pucel, "A General Noise De-embedding Procedure for Packaged Two-Port Linear Active Devices, IEEE Trans. on MTT, Vol.40,
[16] Chin-Hung Chen, "High Frequency Noise modeling of MOSFETs", Master thesis, Simon Fraser University, 1997

Fast noise evaluation: analytical noise model for bipolar transistor

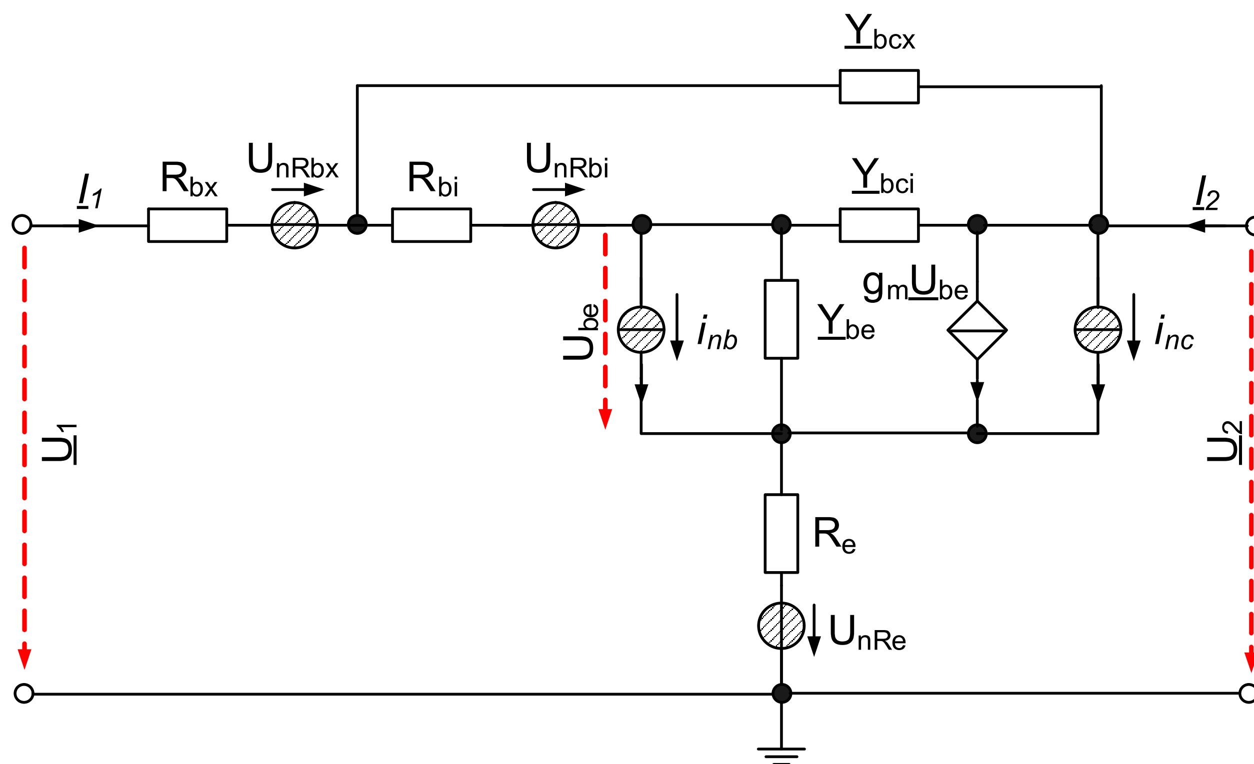

- Noise sources are included: u_{nrbx}, u_{nrbi}, i_{nb}, i_{nc}, u_{nre}
- For noise sources transformation to the input accounts for R_{bx}, R_{bi}, R_e and C_{bcx}.

[21] P.Sakalas, J.Herricht, M.Schröter, P.Zampardi, Y.Zimmermann, F.Korndörfer, A.Simukovič, "Verification of p-Equivalent Circuit based microwave Noise Model on AIIIBV HBTs with Emphasis on HICUM", IEEE MTT, International Microwave Symposium Digest (CD-R), Long Beach, CA, USA, (www.ims2005.org), June 11-17, 2005.

Bipolar transistor noise model equations

- Using Noise theory, developed 1955 by H.Rothe and W.Dalke, Noise Parameters are calculated.

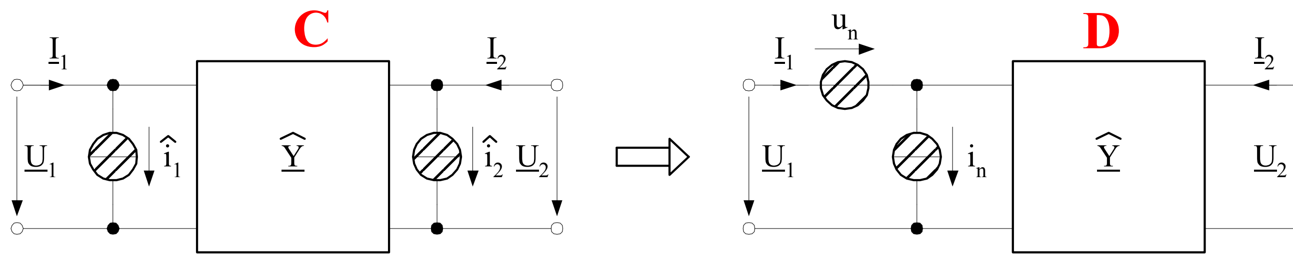

Spectral Densities (SD) of the noise sources in **D** are:

$$S_{u_n} = \frac{1}{|\hat{\underline{Y}}_{21}|^2} S_{i_2} + r_{bx}^2 S_{i_1} + 4kTr_{bx} - 2r_{bx} Re\left\{\frac{1}{\hat{\underline{Y}}_{21}^*} S_{i_1 i_2}\right\}$$

$$S_{i_n} = S_{i_1} + \left|\frac{\hat{\underline{Y}}_{11}}{\hat{\underline{Y}}_{21}}\right| S_{i_2} - 2Re\left\{\frac{\hat{\underline{Y}}_{11}}{\hat{\underline{Y}}_{21}} S_{i_2 i_1}\right\}, \quad S_{i_n u_n} = r_{bx} S_{i_1} + \frac{\hat{\underline{Y}}_{11}}{|\hat{\underline{Y}}_{21}|^2} S_{i_2} - \frac{1}{\hat{\underline{Y}}_{21}^*} S_{i_1 i_2} - r_{rbx} \frac{\hat{\underline{Y}}_{11}}{\hat{\underline{Y}}_{21}} S_{i_2 i_1},$$

$$S_{i_1} = |1 - r_{bi} \tilde{\underline{Y}}_{11}|^2 S_{\tilde{i}_b} + |\tilde{\underline{Y}}_{11}|^2 S_{\tilde{u}_{rbi}}, \quad S_{i_2} = S_{\tilde{i}_c} + r_{bi}^2 |\tilde{\underline{Y}}_{21}|^2 S_{\tilde{i}_b} - 2r_{bi} Re\left\{\tilde{\underline{Y}}_{21} S_{\tilde{i}_b \tilde{i}_c}\right\} + |\tilde{\underline{Y}}_{21}|^2 S_{\tilde{u}_{rbi}}$$

[14] H. Rothe, W. Dahlke, “Theory of Noisy Fourpoles,” Proc. *IRE*, 44, pp.811-818, 1956.
[21] P.Sakalas, J.Herricht, M.Schröter, P.Zampardi, Y.Zimmermann, F.Korndörfer, A.Simukovič, "Verification of p-Equivalent Circuit based microwave Noise Model on AIIIBV HBTs with Emphasis on HICUM", IEEE MTT, International Microwave Symposium Digest (CD-R), Long Beach, CA, USA, (www.ims2005.org), June 11-17, 2005.

Analytical noise model verification on 150 GHz SiGe HBTs

150 GHz process HBTs

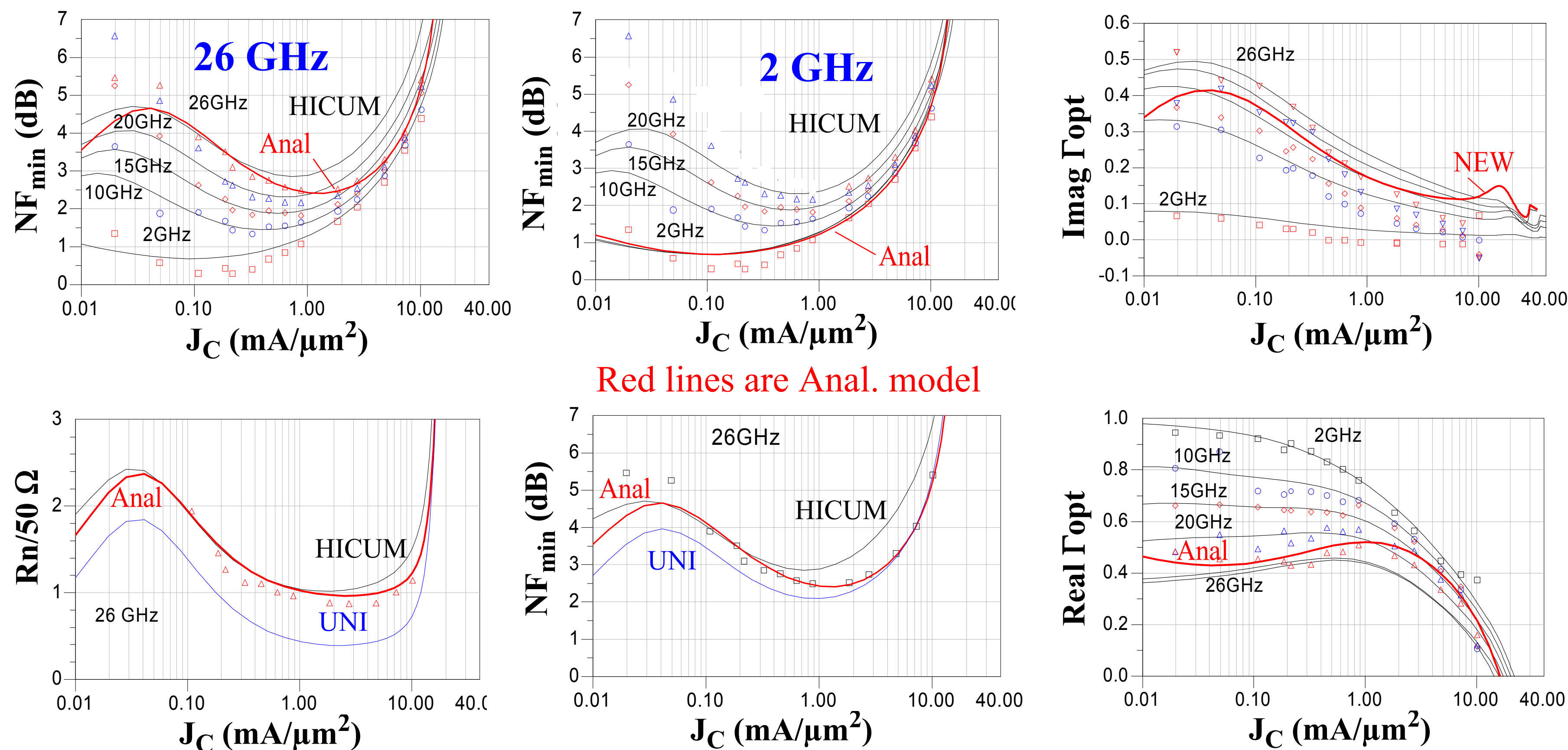

- Analytical noise model is in a good agreement, especially at high current densities and high frequencies. => Reason is correlation impact.
- Other analytical noise models UNI [G.Niu et al, *IEEE ED,* V.48, N.11, 2001] approach is off.

Noise model verification versus frequency

150 GHz process HBTs

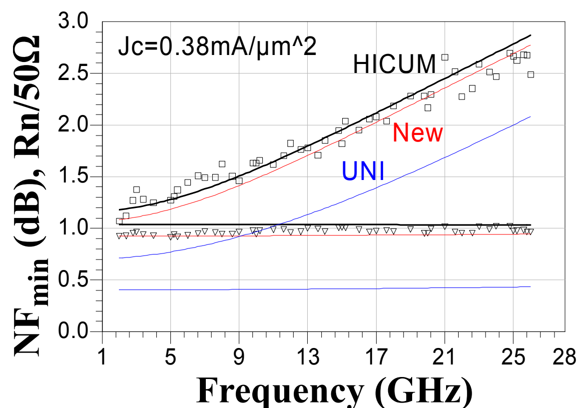

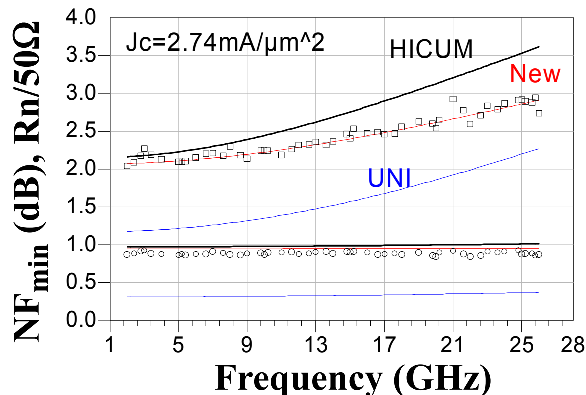

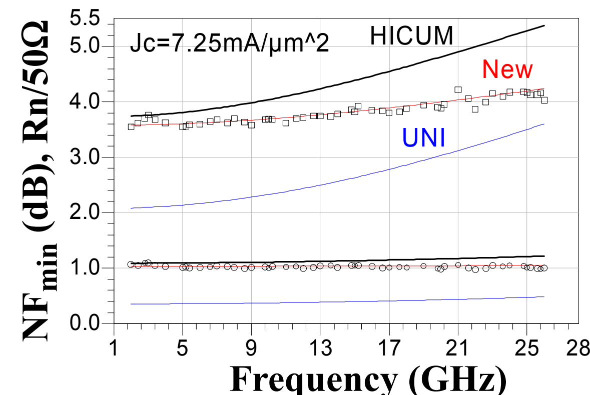

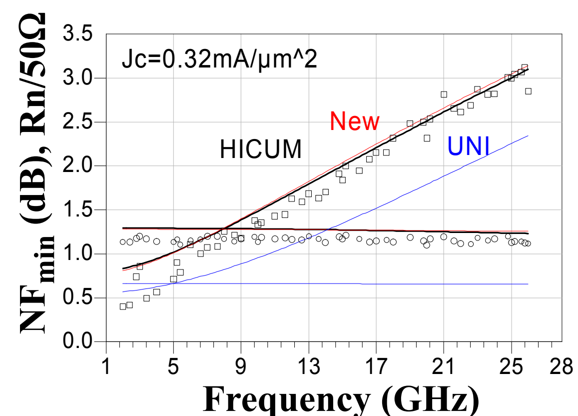

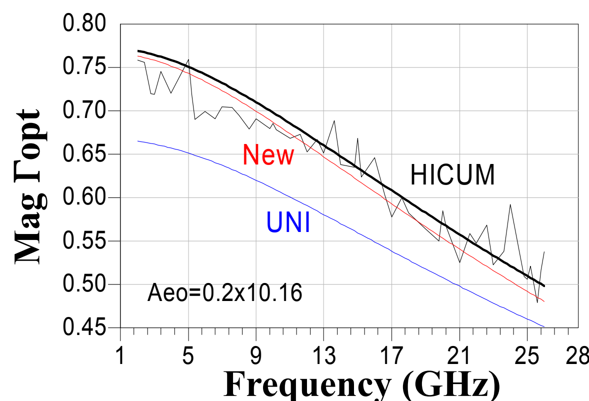

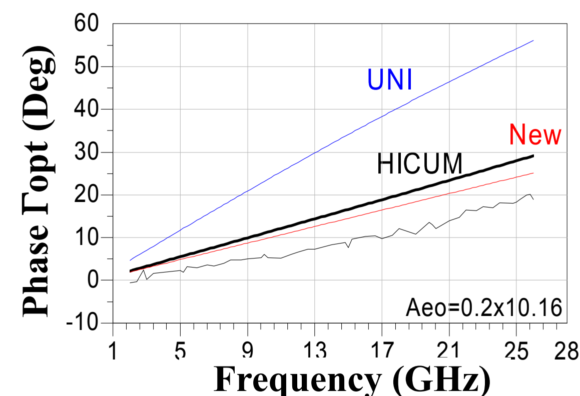

- Cross-correlation accounted by the model with delay time $\tau = 0.19$ ps.
- For $\tau = 0$ ps, noise parameters arrive to CM => shot noise correlation matters.

Compact model HICUM L2 with noise sources

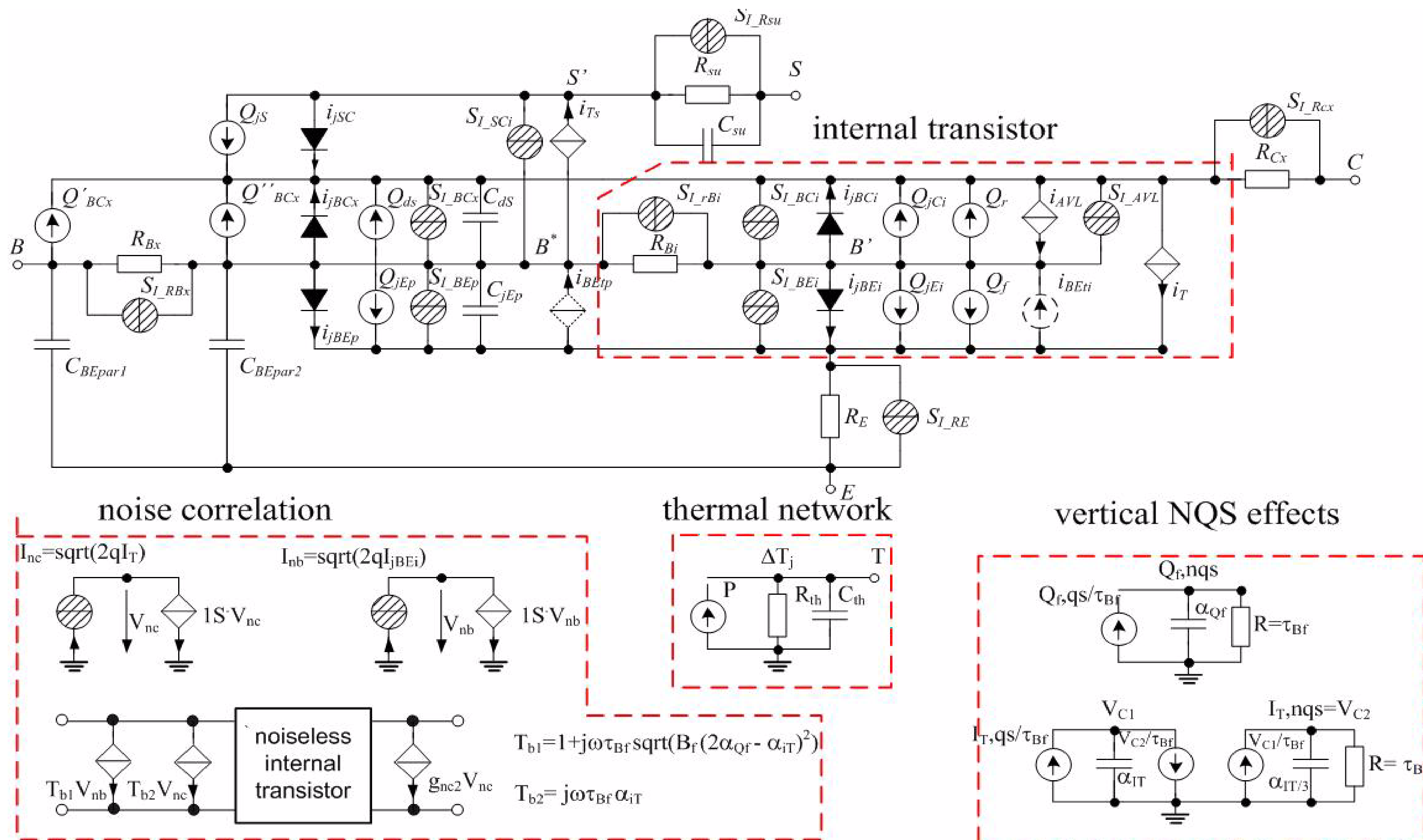

RF and noise parameters over technology node

Investigated SiGe and $A_{III}B_V$ HBTs

Technology	Drawn Emitter Area	f_T, GHz
Atmel LEC	0.5 um x 20.3 um	80
Jazz Semiconductors	0.22 um x 10.16 um	150
IFX Infineon Technologies	0.2 um x 10 um	200
ST Microelectronic	0.13 um x 10.8 um	300
Teledyne inc.	0.25 um x 10 um and other	400
Skyworks inc.	2.2 um x 22 um	50

Noise sources decomposition of NF_{min} for different generation HBTs

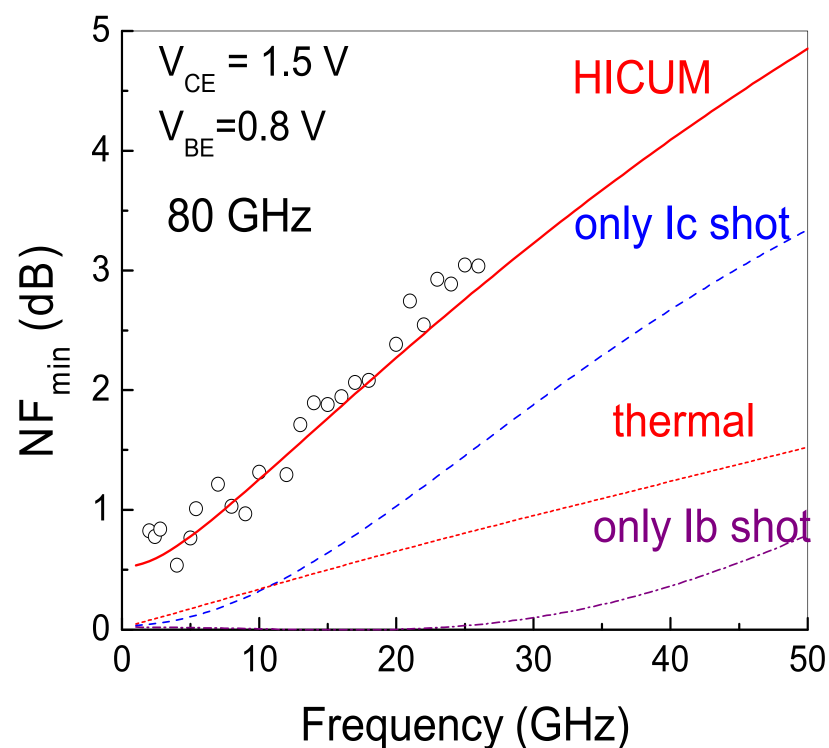

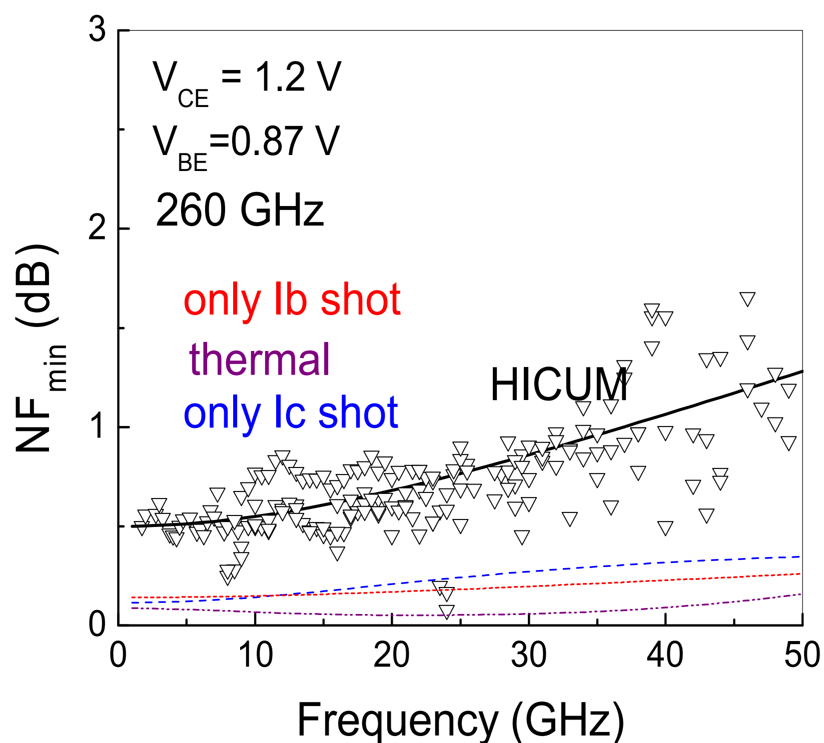

- Decomposed noise superposition is not valid since each internal noise source has different transfer to the input function.
- Decomposition is based on switching different noise sources off in Verilog-a code.

Shot noise correlation in SiGe HBTs, compact model solution and verification

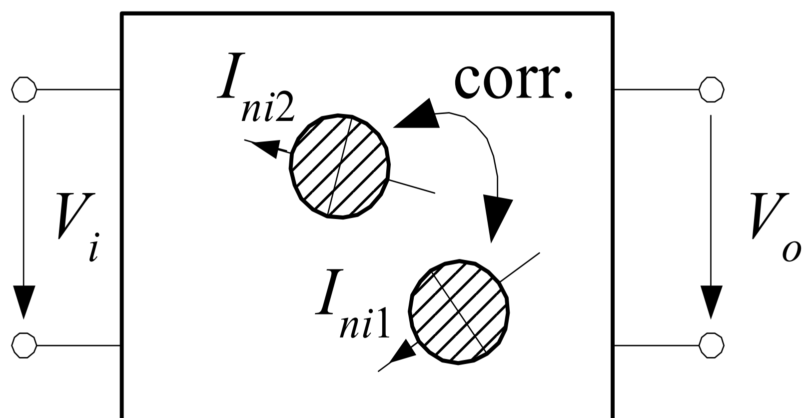

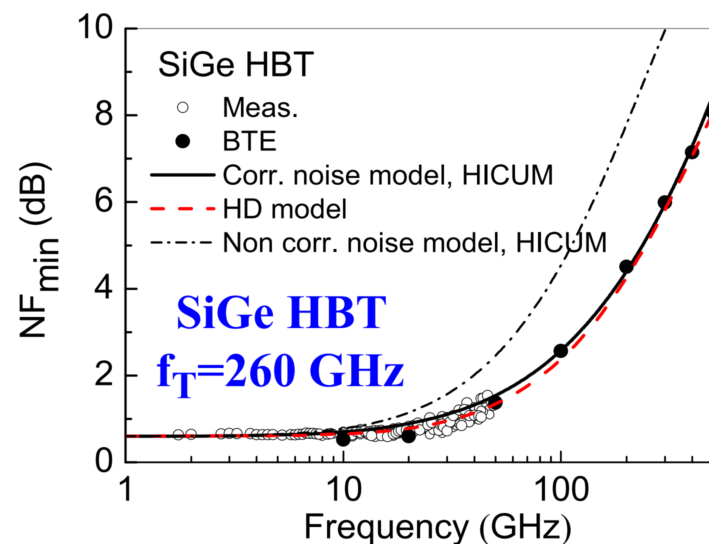

- Collector current shot noise and base dynamic current shot noise are correlated and correlation impacts NF_{min}.
- TCAD simulations (Hidrodynamic model (HD) and Boltzmann Transport Equation (BTE) simulation) show good agreement against measured data.
- Transistor can be treated as two port with internal noise sources, which might be correlated.

[17] J. Herricht, P. Sakalas, M. Ramonas, M. Schröter, C. Jungemann, A. Mukherjee, K. E. Moebus" Systematic Compact Modeling of Correlated Noise in Bipolar Transistors" IEEE Trans on MTT, Vol.60, No.11, 2012, pp. 3403-3411

Shot noise correlation model implementation to compact model

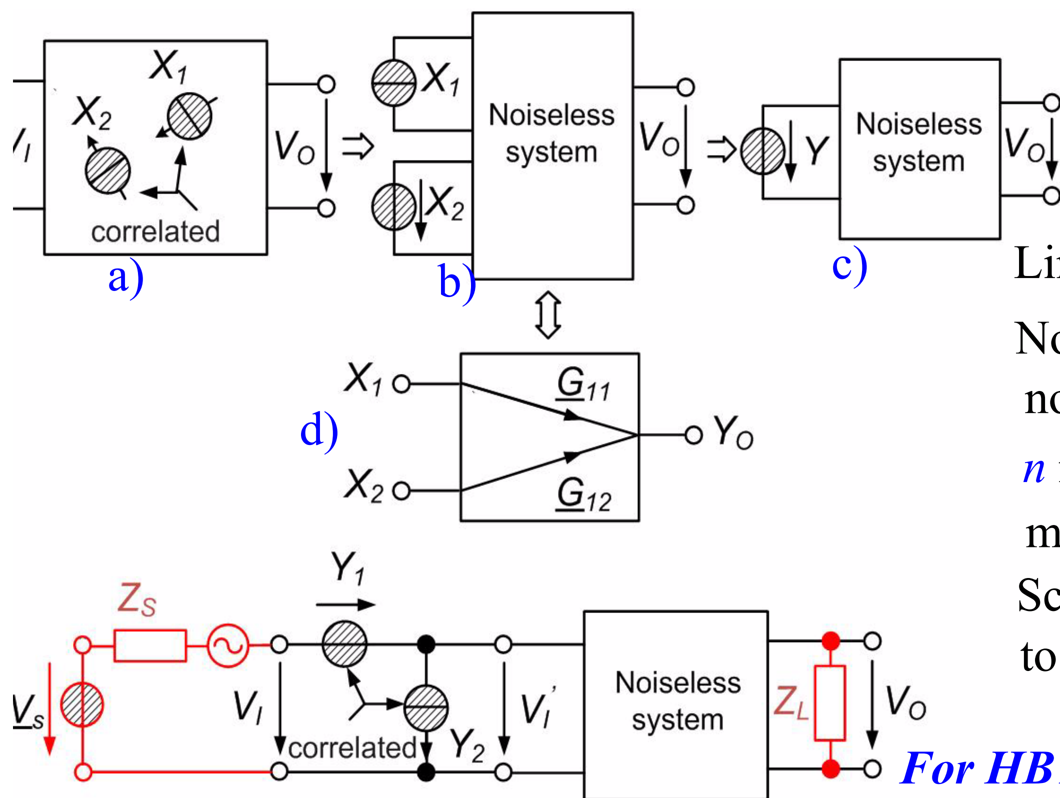

Linear noisy system with n noise sources.

Noise figure calculation requires noise sources at the input.

n noise sources at the input has to be merged to a single noise source.

Schematic of the n noise source linking to a single one with transfer functions $\underline{G}_n$

For HBT we have two correlated noise sources.

- Commercial circuit simulators can handle non-correlated noise sources only. An appropriate transformation (transformation matrix $\mathbf{T}$) has to be derived which converts a network with correlated noise sources x_i into a modified network with non-correlated noise sources $\bar{x}_i$.

[17] J. Herricht, P. Sakalas, M. Ramonas, M. Schröter, C. Jungemann, A. Mukherjee, K. E. Moebus" Systematic Compact Modeling of Correlated Noise in Bipolar Transistors" IEEE Trans on MTT, Vol..60, No.11, 2012, pp. 3403-3411

Graphical interpretation of shot noise correlated compact model

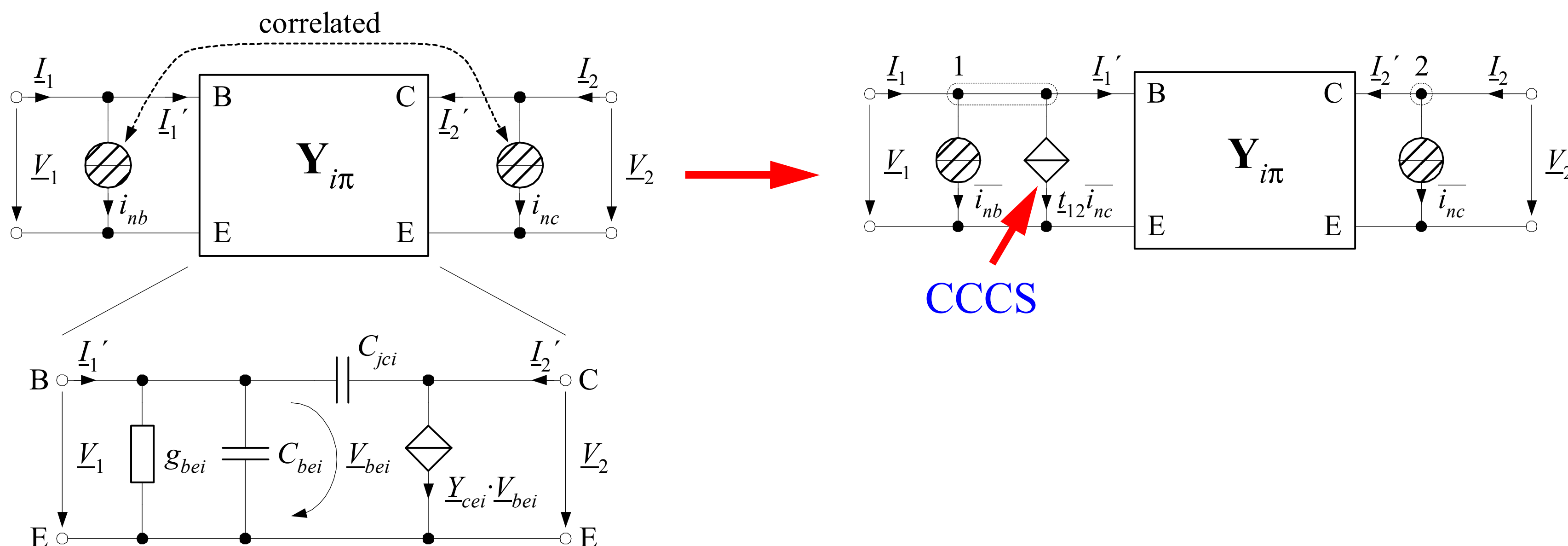

- Adopted for HICUM an internal noise model from Van der Ziel was used:

$$S_{inbinc} = j\omega\tau_{Bf}\alpha_{it}2qI_C \qquad S_{inc} = 2qI_C \qquad S_{inb} = 2qI_B[1 + 2\alpha_{qf}B_f(\omega\tau_{Bf})^2] \ ,$$

where α_{it} ... scaling factor for NQS delay time of the transfer current, τ_{Bf} .. base transit time for active forward operation, α_{qf} ... scaling factor for non-quasi-static (NQS) delay time due to minority charges, B_f ... current gain in common emitter connection, I_B ... base current through BE diode, I_C ... transfer current ($I_C = I_T$).

[17] J. Herricht, P. Sakalas, M. Ramonas, M. Schröter, C. Jungemann, A. Mukherjee, K. E. Moebus" Systematic Compact Modeling of Correlated Noise in Bipolar Transistors" IEEE Trans on MTT, Vol..60, No.11, 2012, pp. 3403-3411

Correlated compact model verification: NF_{min}

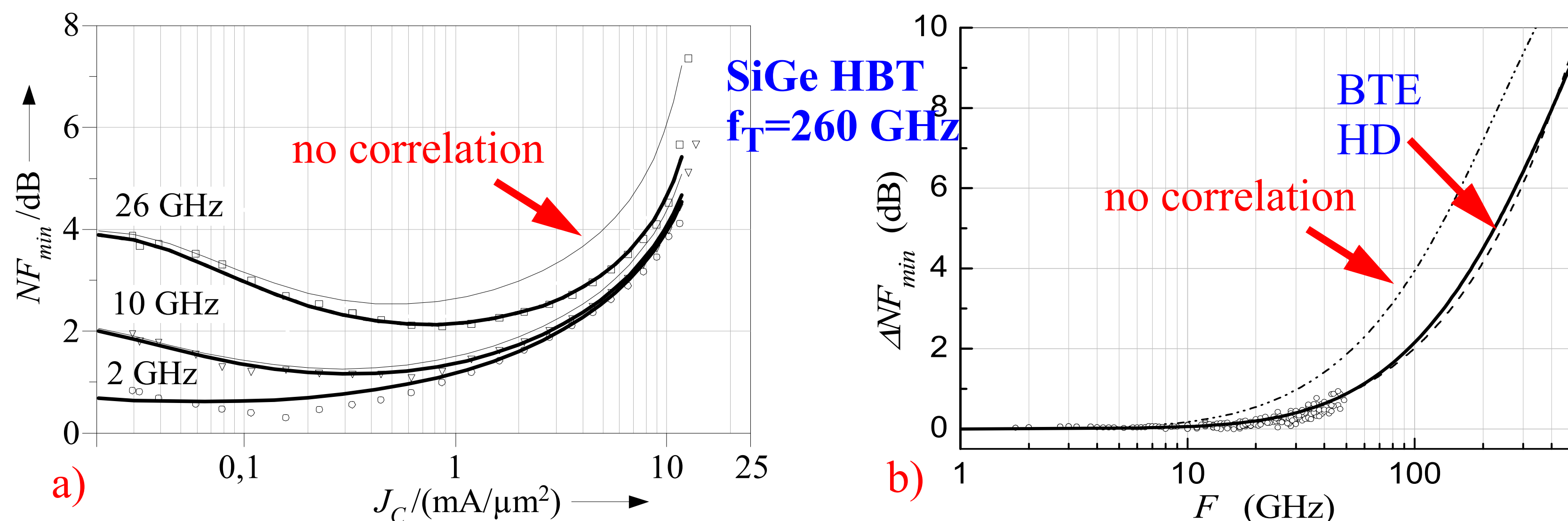

- Compact noise model was verified on various technology HBTs: 80 GHz Atmel, 150 GHz Jazz Semi, 200 GHz IFX Infineon and on ST Microelectronics 260 GHz HBT.
- a) NF_{min} versus current density and frequency for 150 GHz Jazz Semi SiGe HBT. b) ΔNF_{min} for ST Microelectronis SiGe HBT with f_T= 260 GHz are presented.
- Boltzmann transport equation simulation, hidrodynamic model and HICUM are in a perfect agreement with measured data.

[17] J. Herricht, P. Sakalas, M. Ramonas, M. Schröter, C. Jungemann, A. Mukherjee, K. E. Moebus" Systematic Compact Modeling of Correlated Noise in Bipolar Transistors" IEEE Trans on MTT, Vol.60, No.11, 2012, pp. 3403-3411

Correlated compact model verification: Γ_{opt}, f_T

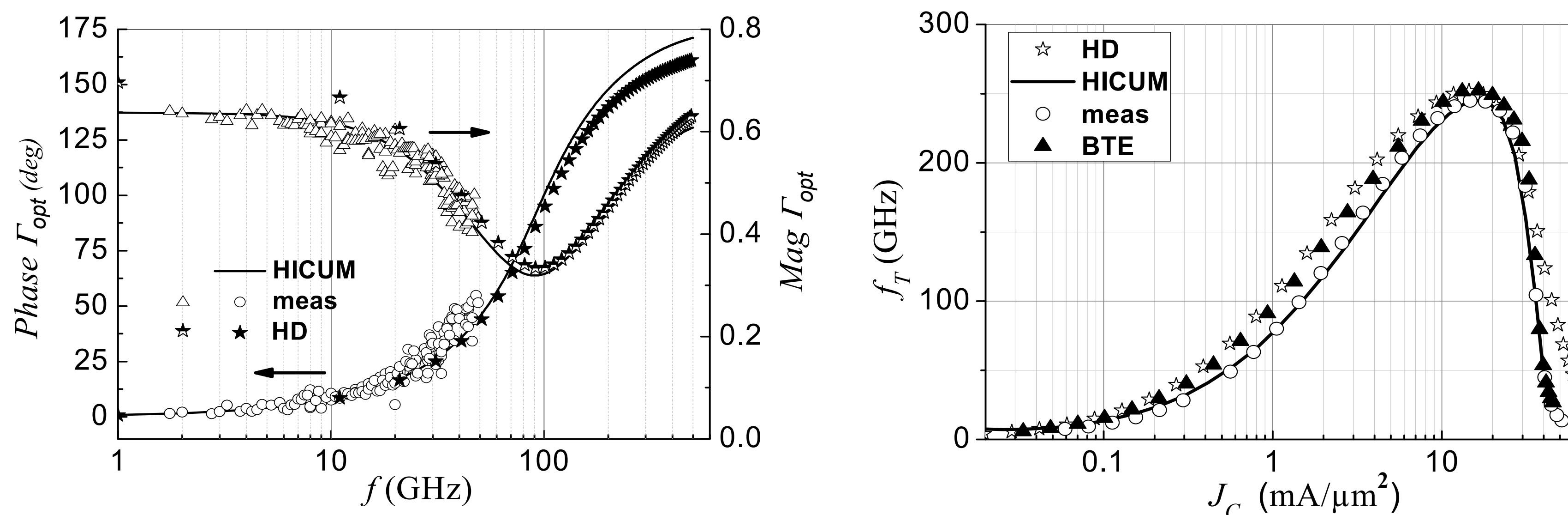

- HICUM is in a perfect agreement with HD and measured data. Correlation has no impact on Γ_{opt}.
- Cut-off frquency for BTE and HD simulation is slightly higher due to missing external parasitics in the TCAD model.

[17] J. Herricht, P. Sakalas, M. Ramonas, M. Schröter, C. Jungemann, A. Mukherjee, K. E. Moebus" Systematic Compact Modeling of Correlated Noise in Bipolar Transistors" IEEE Trans on MTT, Vol.60, No.11, 2012, pp. 3403-3411

Avalanche noise in SiGe HBT: measurement and modeling

Circuit designers usually are trying to avoid device operation at impact ionization (II) bias conditions, where device output conductance is rapidly increased as well as noise is degraded.

Nevertheless in certain applications, such as fiber-optics, drivers for optical modulation, transistors may be pushed to operate at voltages beyond BV_{CE0}.

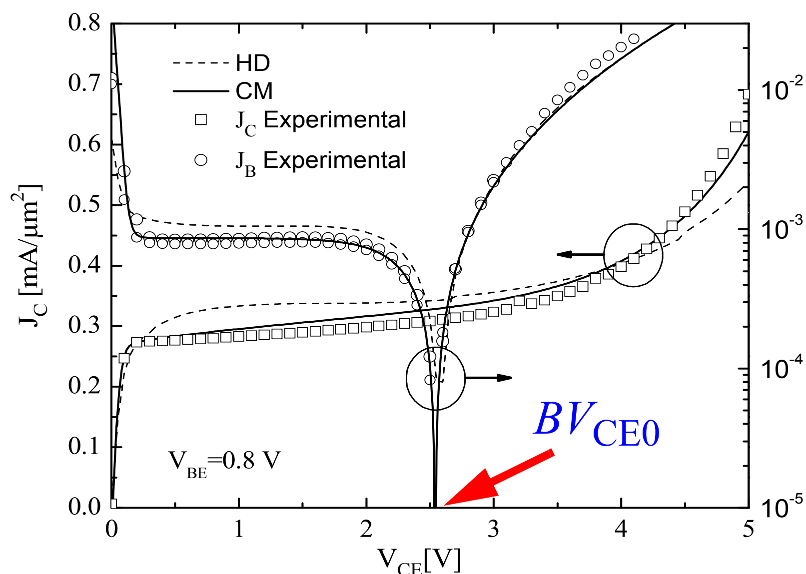

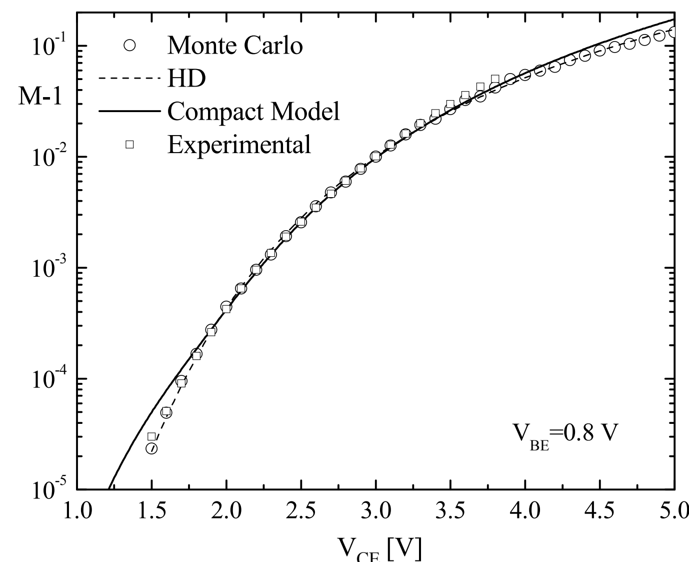

- HICUM, TCAD simulated IV char. and multiplication factor $M-1 = \frac{I_{avl}}{I_T}$.

[18] P. Sakalas, M. Ramonas, M. Schröter, C. Jungemann, A. Shimukovitch, W. Kraus "Impact Ionization Noise in SiGe HBTs: Comparison of Device and Compact Modeling With Experimental Results" in IEEE Trans. on ED,Vol.56,No.2, 2009, pp. 328-336.

Avalanche multiplication noise in SiGe HBT

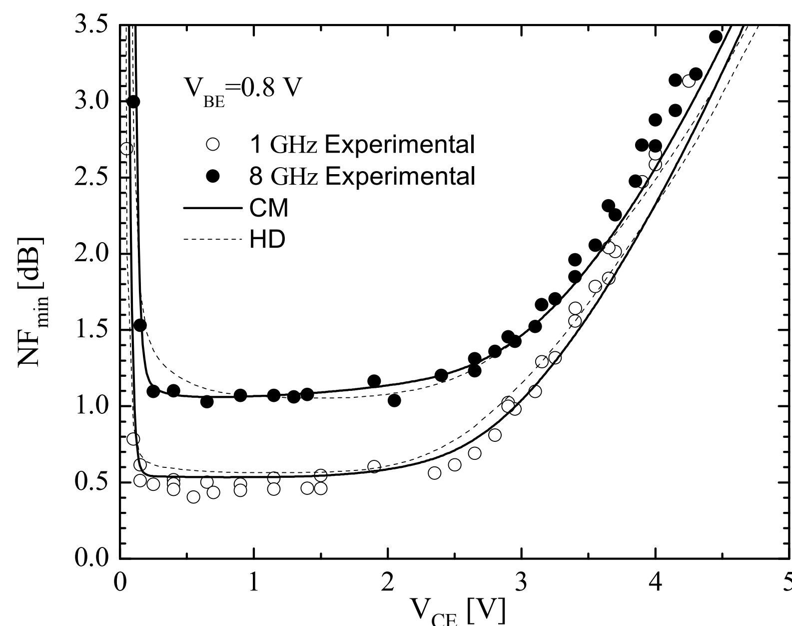

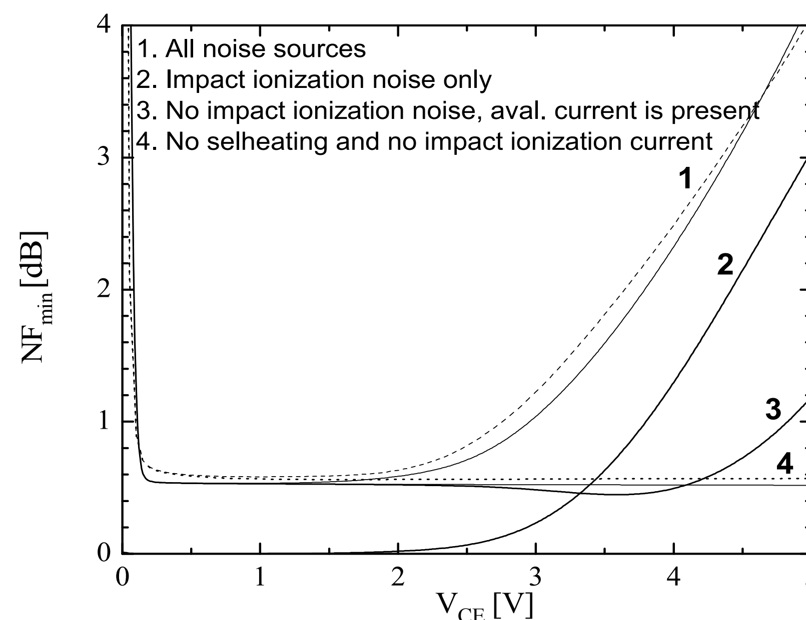

- NF_{min} rise beyond BV_{CE0} is related to avalanche multiplication current related shot noise.
- Turning off the II noise source and keeping the II effect, the avalanche multiplication related collector shot noise amplification leads to a visible increase of NF_{min} (curve 3).

[18] P. Sakalas, M. Ramonas, M. Schröter, C. Jungemann, A. Shimukovitch, W. Kraus "Impact Ionization Noise in SiGe HBTs: Comparison of Device and Compact Modeling With Experimental Results" in IEEE Trans. on ED,Vol.56,No.2, 2009, pp. 328-336.

High frequency noise in InP based HBTs: suitability for LNA?

IV characterisitcs RF performance

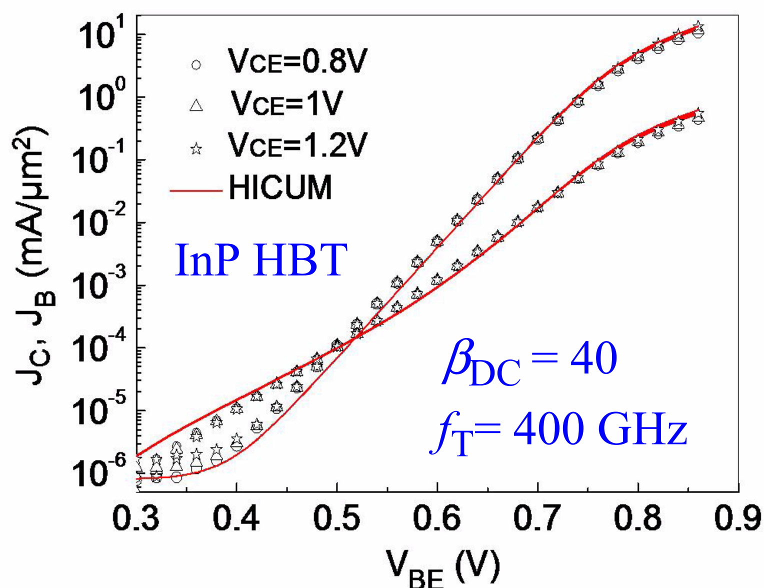

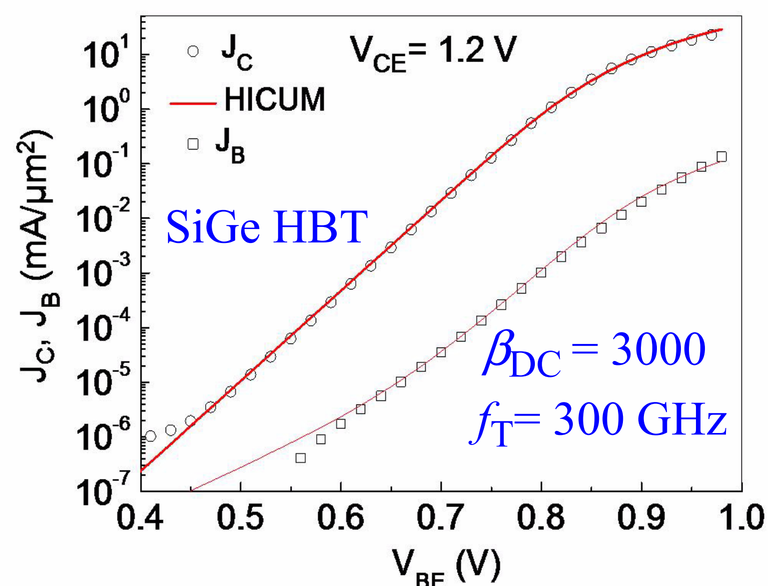

InP DHBTs with a wide bandgap InP collector exhibits high f_T = 0.6 THz simultaneous with high breakdown voltages BV_{CE0} > 4 V, resulting in a record f_T x BV_{CE0} of 2.53 THz V.

- High base doping in InP HBTs results to relatively large recombination current, compared to SiGe HBT and thus lower current gain.
- High base recombination current results to high base shot noise.

[19] P. Sakalas, M. Schroter, H. Zirath "mm-Wave noise modeling in advanced SiGe and InP HBTs" Journal of Computational Electronics 14, DOI 10.1007/s10825-015-0664-6, pp.62–71, 2015

f_T and f_{max} for InP and SiGe HBTs

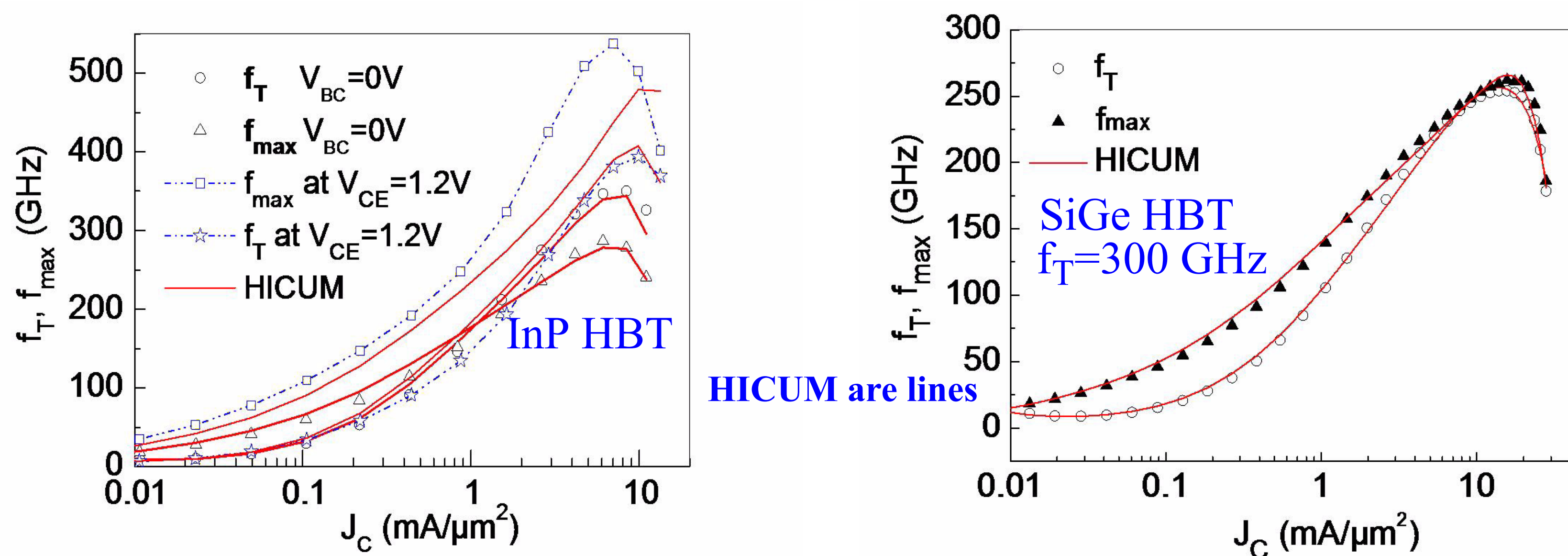

- InP DHBTs with A_{E0} = 0.25 μm x 10 μm exhibit f_T/f_{max} = 400/550 GHz
- Nonequilibrium transport is evident: a sharp increase of f_T and f_{max} with a current density in the J_C range from 0.07 to 10 mA/μm^2 is present, which can not be captured by the model.
- The comparison of τ_{EC} for SiGe and InP HBTs at V_{BC} = 0 V shows that NT effect is present for InP but not for SiGe HBTs.

[19] P. Sakalas, M. Schroter, H. Zirath "mm-Wave noise modeling in advanced SiGe and InP HBTs" Journal of Computational Electronics 14, DOI 10.1007/s10825-015-0664-6, pp.62–71, 2015

High frequency noise in InP and SiGe HBTs

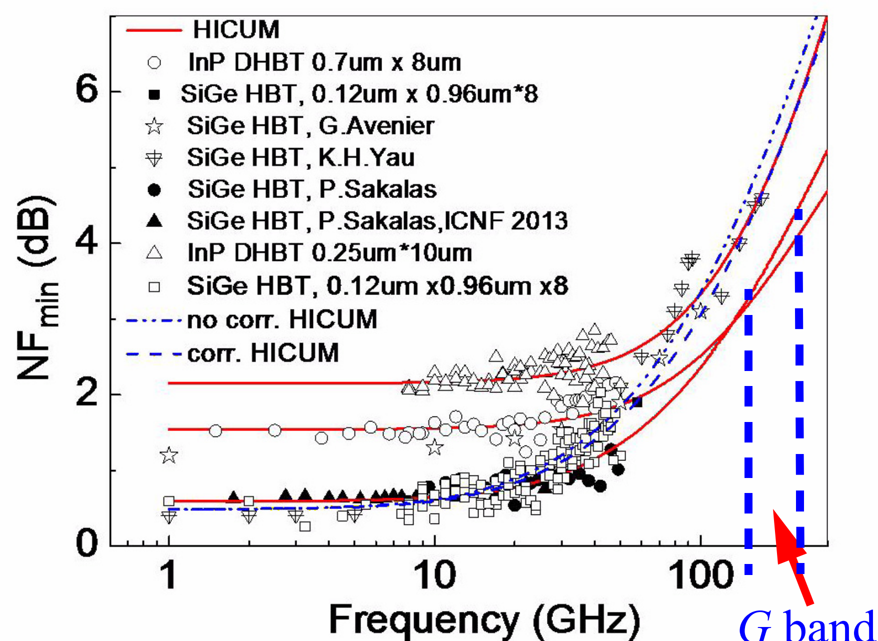

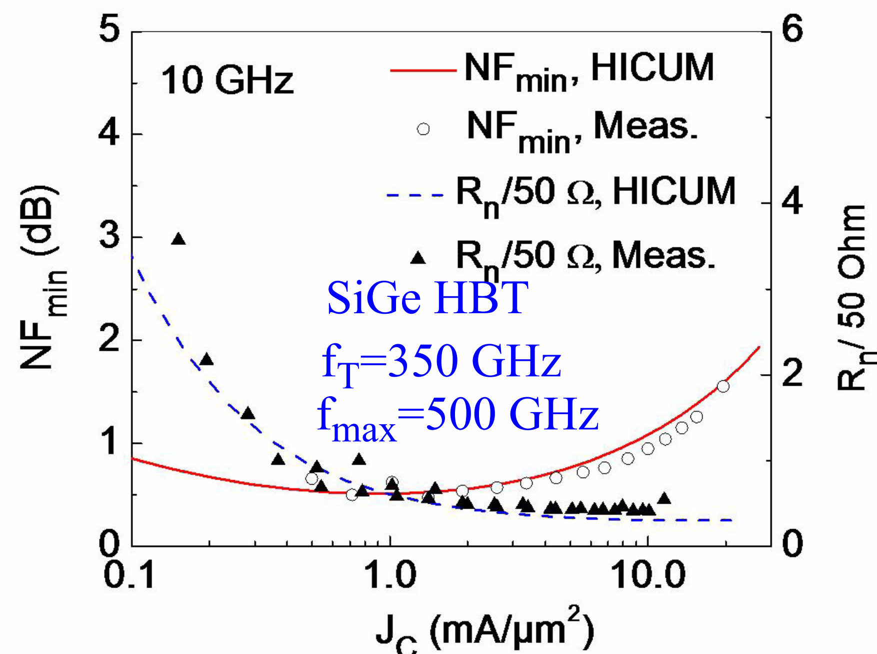

- The comparison shows that the noise properties of InP DHBT due to high RF gain at milli-meter frequencies are comparable to the best low noise high speed SiGe HBTs.
- Shot noise correlation for InP HBT is negligible.

A physics-based compact model allows predictions of the device trend at frequencies where measurements are still impossible.

[19] P. Sakalas, M. Schroter, H. Zirath "mm-Wave noise modeling in advanced SiGe and InP HBTs" Journal of Computational Electronics 14, DOI 10.1007/s10825-015-0664-6, pp.62–71, 2015

High frequency noise in InP HBTs: dependence on emitter width.

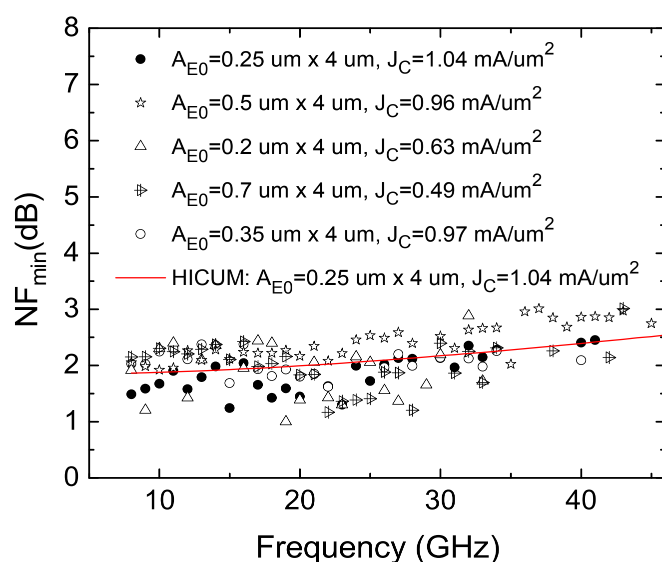

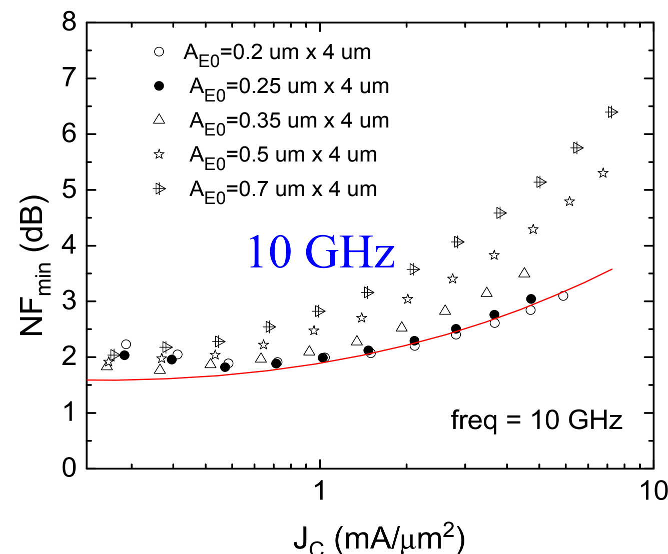

- Same wafer from Teledyne. Noise analysis shows that below 50 GHz InP HBT NF_{min} is shaped by the large base recombination current noise.
- NF_{min} increases with emitter width (f_T = 550 GHz, f_{max} =650 GHz) for A_{E0} = 0.25 x 4.

[19] P. Sakalas, M. Schroter, H. Zirath "mm-Wave noise modeling in advanced SiGe and InP HBTs" Journal of Computational Electronics 14, DOI 10.1007/s10825-015-0664-6, pp.62–71, 2015

[20] P. Sakalas, M. Schröter "Noise in advanced bipolar transistors at mm-wave frequencies" (Invited) Proceedings of the 23rd Int. Conf. on Noise and Fluctuations, Xian, China, June 2-5, 6 p., 2015.

AlGaAs/GaAs and Si/SiGe Band diagram at equilibrium

AlGaAs/GaAs HBT

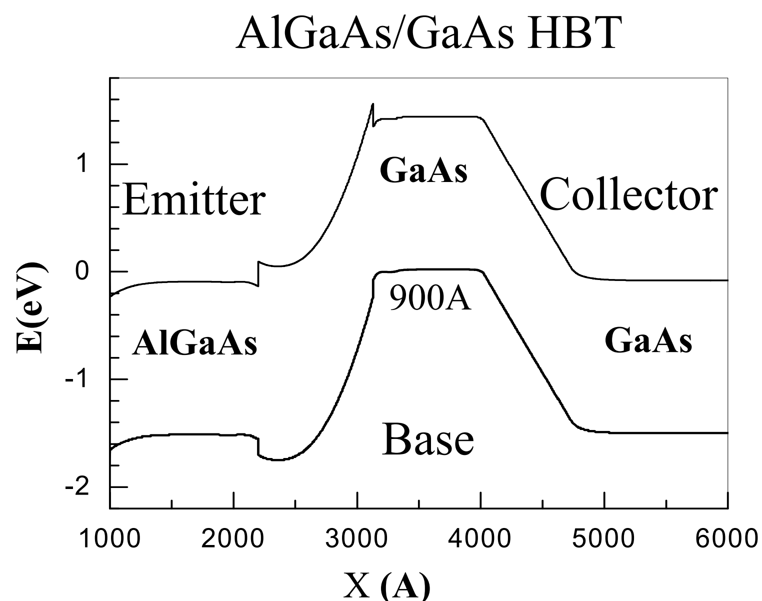

Drift Si/SiGe HBT

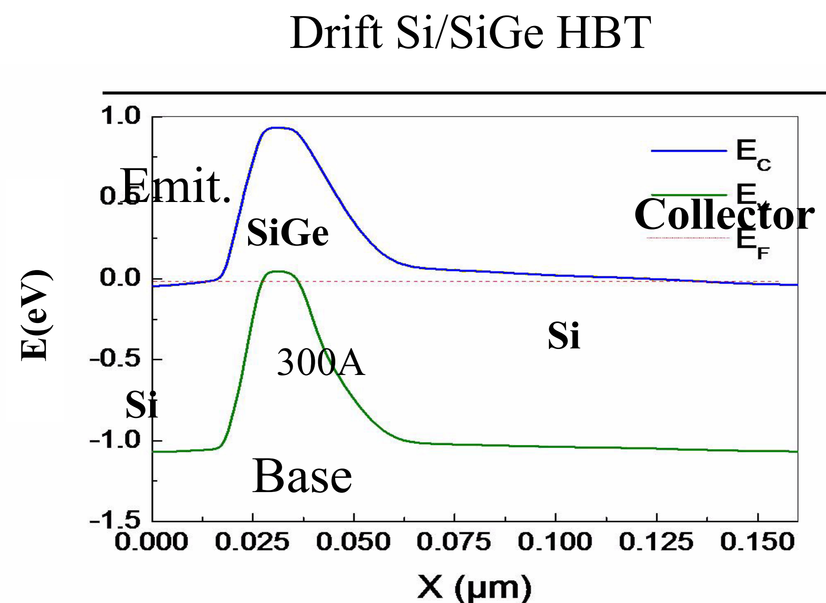

- For AlGaAs/GaAs ΔE~0.37eV

$$\frac{Jn}{Jp} = \frac{DnpLpnNdNcpNvp}{DpnLpnNaNcnNvn} \exp\left[\left(\Delta Wn - \Delta Wp\right)\frac{1}{kT}\right]$$

- =>exp[(ΔWn-ΔWp)/kT] ~6.10[7]=> forward current is determined by the difference of potential barriers ΔW_n-ΔW_p, but not the carrier densities nearby the heterobarrier.
- Higher conduction band discontinuity requires large V_{BE}~1.3 V for to bias AlGaAs-GaAs HBT.
- => electrons enter base from the ramp with high energy causing quasiballistic motion in the base.

GaAs HBT: transit time, f_T, NF_{min} dependence on base layer thickness, doping.

GaAs based HBT: layers thicknesses, doping.

InGaAs	N	$>1*10^{19}$	100 nm	
GaAs	N	$5*10^{18}$	120 nm	
InGaP	n	$3*10^{17}$	40 nm	emitter
GaAs	p+	N_A	50,70,90 nm	base, with different w_b
GaAs	n	$3*10^{16}$	30 nm	collector
Spike	n	$2*10^{18}$	5 nm	δ layer for CCHBT
InGaP	n	$3*10^{16}$	10 nm	collector layers
GaAs	n	$3*10^{16}/7.5*10^{15}$	155/400 nm	
GaAs	n	$5*10^{18}$	1000 nm	sub-collector

- InGaP/GaAs HBTs with different base layer thicknesses and doping were investigated.
- The target is to investigate impact of base transit time on noise for devices with energy ramp.
- The compound collector CCHBT were analyzed for comparisson.

[22] A. Shimukovitch, P. Sakalas, P. Zampardi, M. Schröter and A. Matulionis "Investigation of electron delay in the base on noise performance in InGaP heterojunction bipolar transistors" Phys. Status Solidi RRL 4, No. 11, 335–337 (2010) / DOI 10.1002/pssr.201004340

GaAs HBT: Gummel plot, f_T.

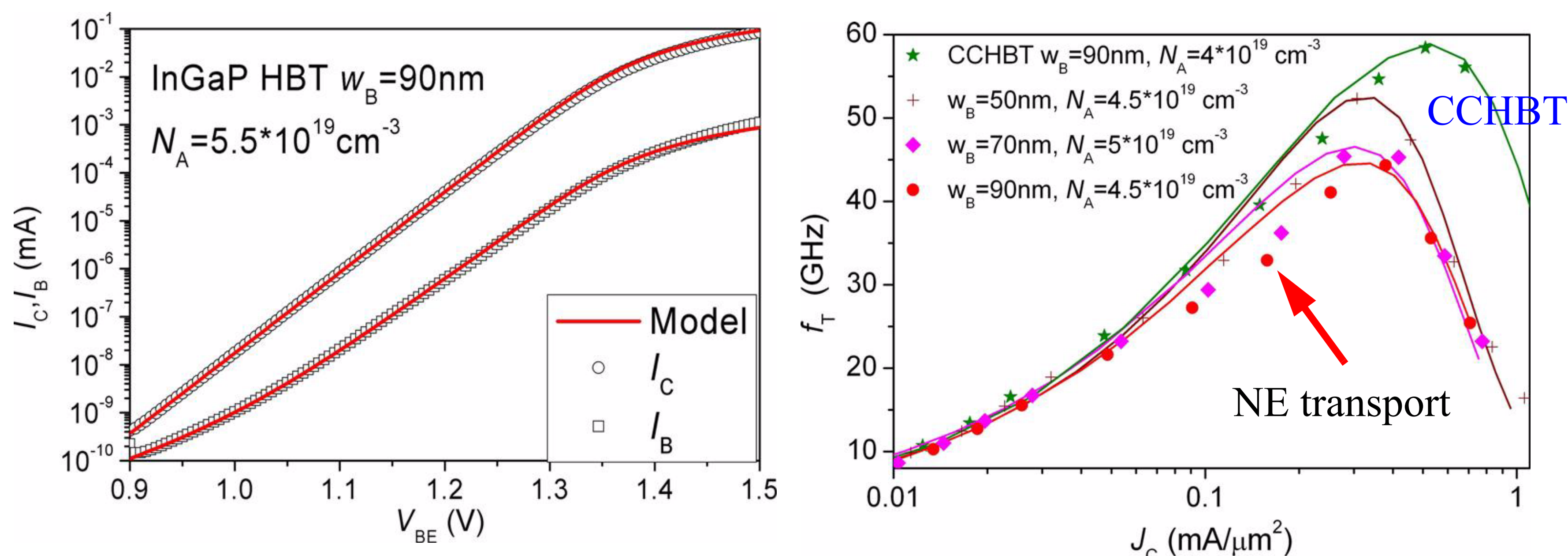

- Forward Gummel plot of GaAs HBT with A_{E0} = 2.2 um x 22 um. HICUM matches measured data for all DC characteristics.
- Nonequilibrium transport (NE) is observed in f_T. CM can not handle it.
- Compound collector (CCHBT) exhibit better performance due to lower accumulated charge in Base/Collector region.

[22] A. Shimukovitch, P. Sakalas, P. Zampardi, M. Schröter and A. Matulionis "Investigation of electron delay in the base on noise performance in InGaP heterojunction bipolar transistors" Phys. Status Solidi RRL 4, No. 11, 335–337 (2010) / DOI 10.1002/pssr.201004340

GaAs HBT: NF_{min} dependence on base layer thickness

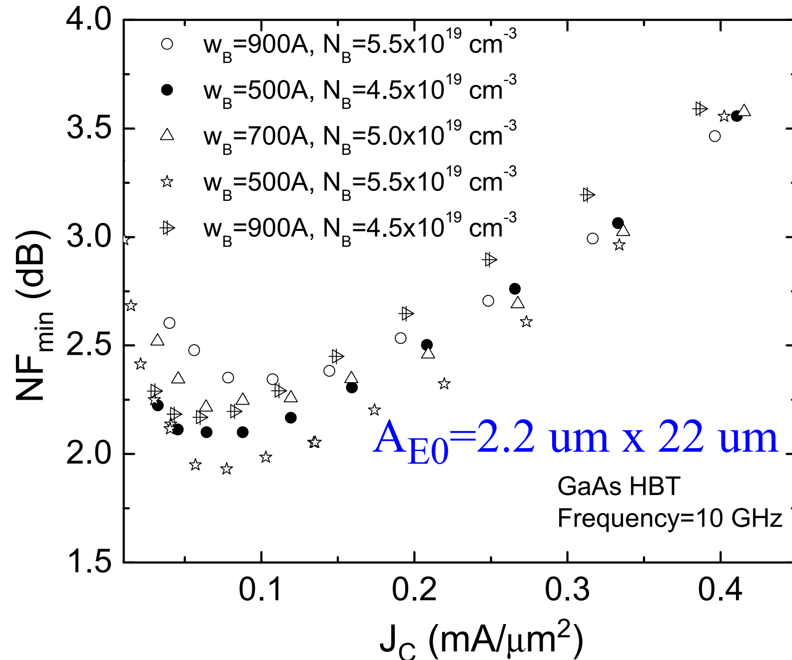

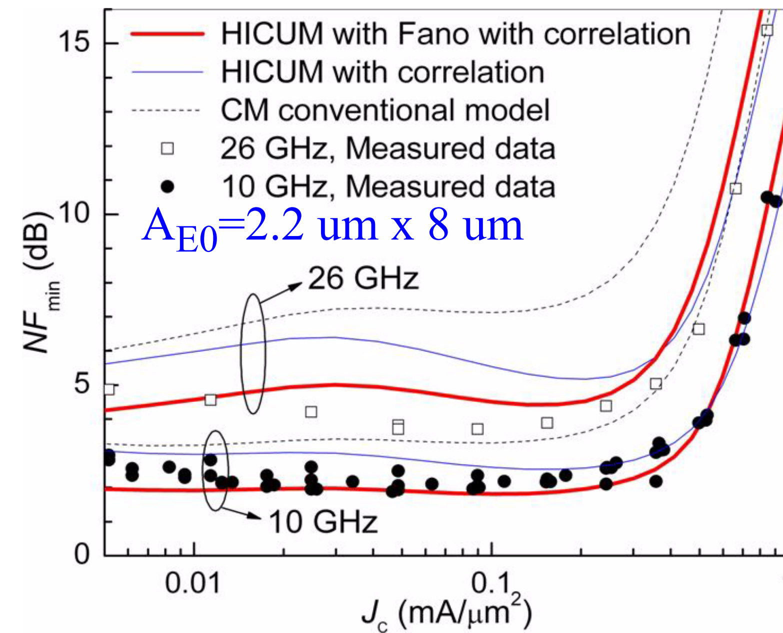

- Slightly better noise performance of GaAs HBT with A_{E0} = 2.2 um x 22 um with base layer width of 500 Angstrom and doping 5.5 x 10^{19} cm^{-3}. Faster base transfer better f_T and better NF_{min}. Effect is not so evident as expected if base transit time matters f_T and NF_{min}!
- => Base transit time is not the main factor reducing the speed of GaAs HBT. Accumulated charge due to NE transport is the main reason for the f_T limitation.

GaAs HBT: NE impact on NF_{min}

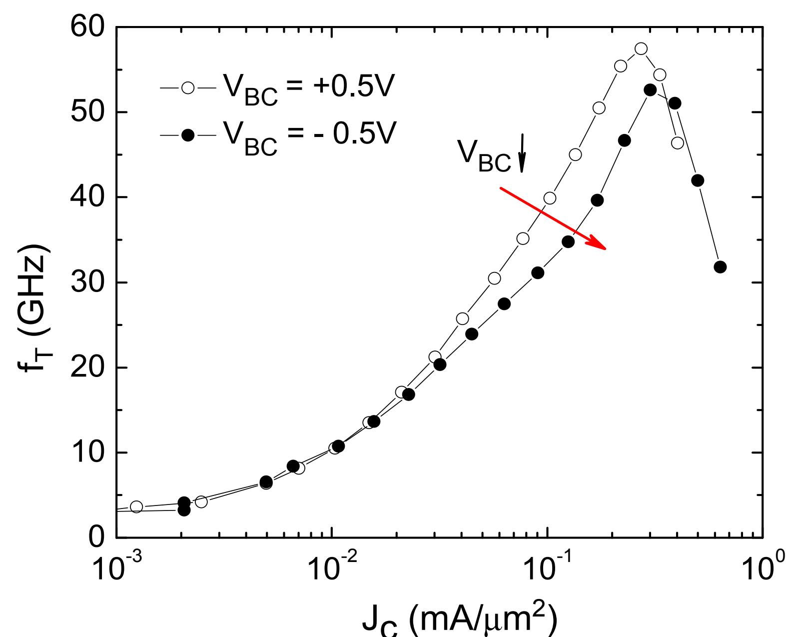

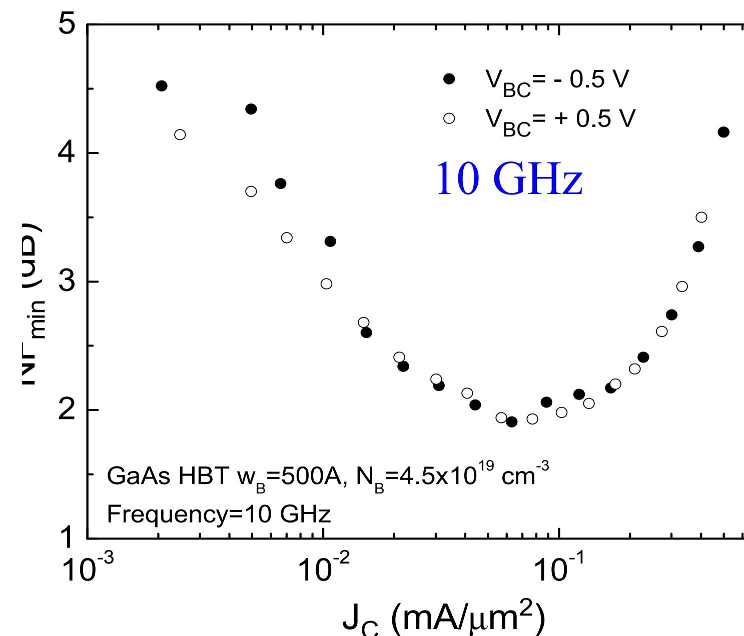

- Increase of negative V_{BC} bias increases electric field in base-collector region and stimulates NE transport. f_T is getting sharper around J_C = 10-1 mA/ um^2.
- Nevertheless impact on NF_{min} at 10 GHz is negligible. As it is seen from the model (previous slide a signifficant impact is observed at 26 GHz.

Shot noise suppression

Extracted Spectral densities of base and collector current shot noise.

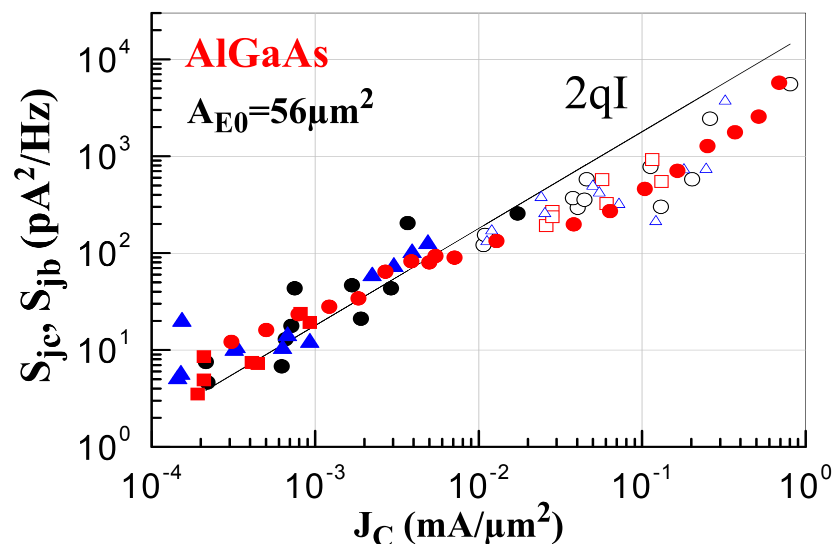

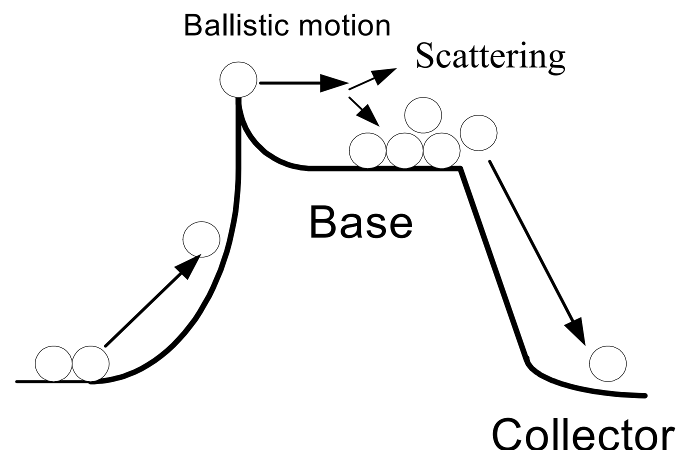

- Shot noise suppression in GaAs HBTs: => High energy electrons emitted via ramp of emitter/base junction discontinuity after ballistic movement are being randomized by ionized impurity and optical phonon scattering events. This results to the formation of the space charge region which screens the transfer of electrons via E/B junction and thus supress related shot noise.
- High energy electrons in the collector can reach intervalley (*IV*) phonon energy and emit *IV* phonon. Very intensive *IV* scattering related noise might be present in the collector epilayer.

Intervalley noise impact to NF_{min}?

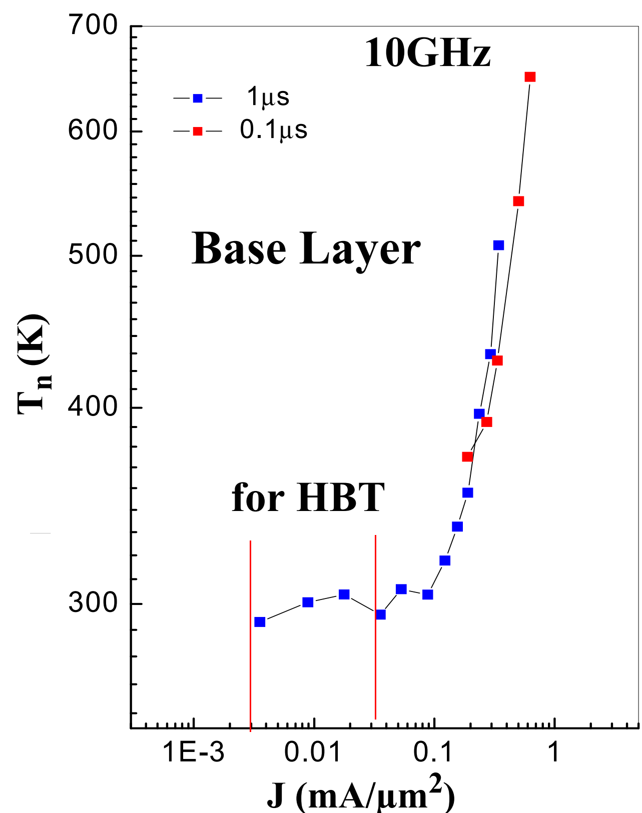

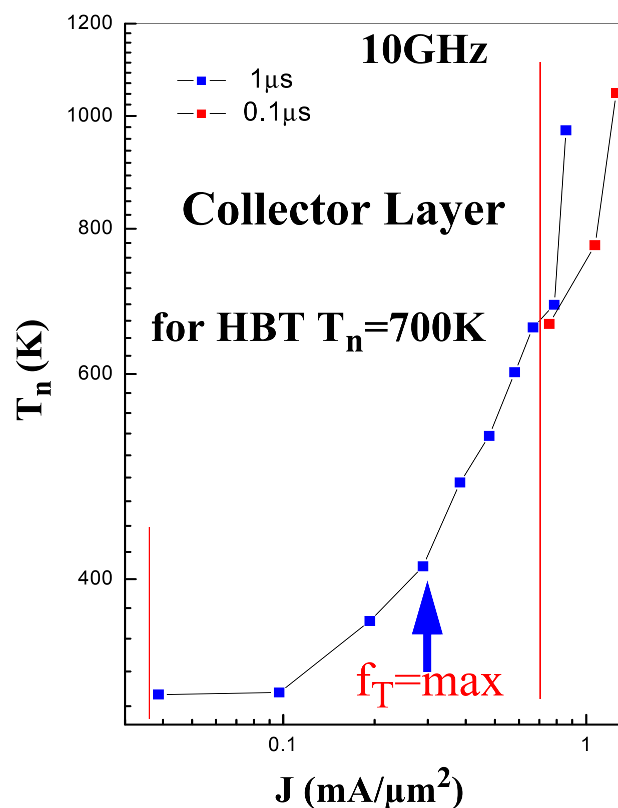

Gated
Noise measurement

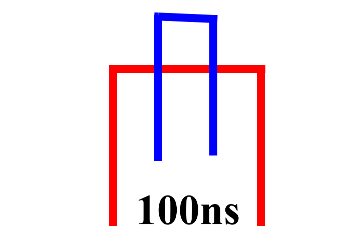

Bias Pulse Duration measurement.
125 Hz repetition.

- Hot hole noise in the base is negligible.
- Hot electron noise in collector layer can reach up to 700 K:
  - **Impact on NF_{min}:** => ~0.1 dB increase at high frequencies only.

Acknowledgement

Michael Schroter is acknowledged for inspiration and tireless discussions. Jorg Herricht is acknowledged for the support with correlated model implementation and numerous derivations, Tobias Nardmann and Andreas Pawlak are acknowledged for discussions and support with HICUM parameter extraction, all from CEDIC TU Dresden I am thankfull to Mindaugas Ramonas from FMTC Lithuania for the support with TCAD simulations.
Min Zhang from SIMTAC (China) is acknowlwdged for the possibility to give this presentation.
Andreas Berdzentis from Cascade Microtech is acknowledged for constant support with probes and other available technical support.